

## Two-dimensional $SU(N) \times SU(N)$ chiral models on the lattice. II. The Green's function

Paolo Rossi and Ettore Vicari

*Dipartimento di Fisica dell'Università and I.N.F.N., I-56126 Pisa, Italy*

(Received 25 January 1994)

Analytical and numerical methods are applied to principal chiral models on a two-dimensional lattice and their predictions are tested and compared. New techniques for the strong coupling expansion of  $SU(N)$  models are developed and applied to the evaluation of the two-point correlation function. The momentum-space lattice propagator is constructed with precision  $O(\beta^{10})$  and an evaluation of the correlation length is obtained for several different definitions. Three-loop weak coupling contributions to the internal energy and to the lattice  $\beta$  and  $\gamma$  functions are evaluated for all  $N$ , and the effect of adopting the "energy" definition of temperature is computed with the same precision. Renormalization-group-improved predictions for the two-point Green's function in the weak coupling (continuum) regime are obtained and successfully compared with Monte Carlo data. We find that strong coupling is predictive up to a point where asymptotic scaling in the energy scheme is observed. Continuum physics is insensitive to the effects of the large  $N$  phase transition occurring in the lattice model. Universality in  $N$  is already well established for  $N \gtrsim 10$  and the large  $N$  physics is well described by a "hadronization" picture.

PACS number(s): 11.15.Ha, 11.15.Pg, 75.10.Hk

### I. INTRODUCTION

The study of two-dimensional  $SU(N) \times SU(N)$  principal chiral models is strongly motivated by the deep analogies between this class of field theories and four-dimensional non-Abelian gauge theories. We only mention here asymptotic freedom and the existence of a large  $N$  limit that can be represented as a sum over planar diagrams. A standard lattice version of the continuum action

$$S = \int d^2x \frac{1}{T} \text{Tr} \partial_\mu U(x) \partial_\mu U^\dagger(x) \quad (1)$$

is obtained by introducing a nearest-neighbor interaction

$$S_L = -2N\beta \sum_{n,\mu} \text{Re Tr} [U_n U_{n+\mu}^\dagger], \quad \beta = \frac{1}{NT}. \quad (2)$$

No exact solution of these models is known, even in the large  $N$  limit. An exact  $S$  matrix has however been conjectured [1–3], and numerical evidence seems to indicate that the corresponding bound state spectrum is reproduced in the continuum limit [4]. Also the mass- $\Lambda$  parameter ratio has been conjectured by using the Bethe ansatz approach, and the result is [5]

$$R_{\overline{\text{MS}}} \equiv \frac{M}{\Lambda_{\overline{\text{MS}}}} = \sqrt{\frac{8\pi}{e}} \frac{\sin \pi/N}{\pi/N}, \quad (3)$$

where  $\overline{\text{MS}}$  denotes the modified minimal-subtraction scheme.

Information coming from the  $S$  matrix and large  $N$  factorization leads to the conclusion that when  $N \rightarrow \infty$  principal chiral models are just free field theory in disguise. In other words, a local nonlinear mapping should exist between the Lagrangian fields  $U$  and some Gaussian

variables [6]. The nontriviality of the realization may however be appreciated when considering the two-point Green's function of the Lagrangian field: While at small Euclidean momenta there is substantial evidence for an essentially Gaussian (free field) behavior, at large momenta, where results from standard weak coupling perturbation theory are expected to hold by asymptotic freedom, the Lagrangian field seems to behave more like a composite object formed by two elementary (Gaussian) excitations, which cannot however appear like deconfined free particles. This elementary "hadronization" picture, where however the Lagrangian fields themselves play the role of hadrons, is strongly supported by all numerical evidence that we have produced, and for  $N \gtrsim 6$  is universal, i.e., independent of  $N$ , which confirms that the  $1/N$  expansion, were it available, would be an extremely predictive tool in the analysis of these models.

In the persistent absence of such an expansion, we here tried to apply all other analytical and numerical methods of lattice field theory that seemed appropriate to the problem at hand. In particular we systematically extended the strong coupling character expansion to  $SU(N)$  groups, generating compact formulas for many "standard" integrals and character coefficients and extending the series for the free and internal energy, the magnetic susceptibility, and various definitions of the mass gap. Since principal chiral models possess a wide scaling window in the strong coupling domain, these results become a powerful tool for the analytic computation of physical (continuum) quantities with very small systematic error due to scaling violations.

We also performed many three-loop weak coupling lattice computations in order to improve our understanding of the approach to asymptotic scaling. We found that introducing a new coupling  $T_E$  proportional to the energy [7], the so-called "energy" variable, allows an amazingly

impressive improvement in the convergence of lattice results towards the continuum “asymptotic scaling” predictions, not only when considering such ratios as  $M/\Lambda_L$ , but also when parametrizing the running coupling dependence of the two-point Green’s function in the large momentum regime.

Some of the numerical and analytical results presented here were announced (and presented without proof) in our Refs. [4, 8]. The study of the two-point Green’s function in turn is fully original and constitutes another impressive test of scaling and universality in the context of large  $N$  principal chiral models.

This paper is organized as follows.

In Sec. II we describe a new technique for the strong coupling expansion of  $SU(N)$  models. The strong coupling series of the free-energy density is calculated up to  $O(\beta^{14})$  for  $N > 7$ .

In Sec. III we apply our new technique to the evaluation of the two-point correlation function. Strong coupling series of several different definitions of correlation length are presented.

In Sec. IV we compute the three-loop weak coupling contributions to the internal energy, and to the lattice  $\beta$  function and anomalous dimension of the fundamental field. The corresponding quantities in the energy scheme are also calculated. Continuum predictions for the two-point correlation function are obtained by solving the corresponding renormalization group equation.

In Sec. V we present the results of Monte Carlo simulations for several large values of  $N$ , and compare them to our analytical (strong and weak coupling) calculations.

## II. STRONG COUPLING EXPANSION OF $SU(N)$ MODELS

As stated in the Introduction, a renewed interest in the strong coupling expansion of chiral models was stimulated by the observation of precocious scaling well within the expected convergence radius of the strong coupling series [4], and by the relevance of the complex  $\beta$  singularities of the partition function close to the real axis [9].

Strong coupling in matrix-valued lattice models was pioneered many years ago by several authors. Most studies were however addressed to the (relatively simpler) problem of computing  $U(N)$  group integrals [10–13], while not many results are available concerning  $SU(N)$  integration [14–16]. Moreover, while very general compact formulas can sometimes be written, often these formulas require a lot of supplementary work in order to extract the directly relevant information. Alternatively, tables of numerical coefficients can be routinely generated by computer programs [17], but generality of the results is completely lost. In the search for sufficiently general, but at the same time manageable results we tried to follow a pathway originally opened in Refs. [18–20], whose notation we shall try to follow as far as possible.

We shall focus on the free-energy density of the one-dimensional  $SU(N) \times SU(N)$  chiral model, which can be reinterpreted as a generating functional for  $SU(N)$  group integral in the “standard form”

$$S_{p,q} = \int dU (\text{Tr } U)^p (\text{Tr } U^\dagger)^q, \quad (4)$$

where  $dU$  is the normalized Haar measure for  $SU(N)$ . According to the definitions, the free-energy density  $F$  can be obtained from evaluating

$$\exp[F(\beta)] = \int dU \exp[N\beta (\text{Tr } U + \text{Tr } U^\dagger)]. \quad (5)$$

In turn knowledge of  $F$  allows the knowledge of the coefficients  $z_{(r)}(\beta)$  of the character expansion of the integrand:

$$\begin{aligned} & \exp[N\beta (\text{Tr } U + \text{Tr } U^\dagger)] \\ &= \exp[F(\beta)] \sum_{(r)} d_{(r)} z_{(r)} \chi_{(r)}(U), \end{aligned} \quad (6)$$

where  $\sum_{(r)}$  is a sum over all finite dimensional irreducible representations of the group and  $\chi_{(r)}$  and  $d_{(r)}$  are the corresponding characters and dimensions. Let us now recall from Ref. [19] a few exact results concerning the  $U(N)$  integration. If we denote by

$$A_{m,N} \equiv \det[I_{m+i-j}(s)], \quad (7)$$

where  $I_l$  are the modified Bessel functions and  $s = 2N\beta$ , we find that

$$\tilde{F}_N(\beta) = \ln A_{0,N}(s), \quad (8)$$

$$\Delta_{m,N}(\beta) \equiv \langle [\det U]^m \rangle = \frac{A_{m,N}}{A_{0,N}}, \quad (9)$$

and the following nonlinear ordinary differential equations are satisfied:

$$\begin{aligned} & \frac{1}{s} \frac{d}{ds} s \frac{d}{ds} \Delta_{1,N} + \frac{1}{1 - \Delta_{1,N}^2} \left[ \left( \frac{d\Delta_{1,N}}{ds} \right)^2 - \frac{N^2}{s^2} \right] \Delta_{1,N} \\ & + (1 - \Delta_{1,N}^2) \Delta_{1,N} = 0, \end{aligned} \quad (10)$$

$$\begin{aligned} & \frac{d}{ds} (\ln \tilde{F}_N - \ln \tilde{F}_{N-1}) \\ &= \frac{\Delta_{1,N}}{1 - \Delta_{1,N}^2} \left( \frac{d\Delta_{1,N}}{ds} + \frac{N}{s} \Delta_{1,N} \right). \end{aligned} \quad (11)$$

Moreover [20],

$$\begin{aligned} & \Delta_{m,N}^2 - \Delta_{m+1,N} \Delta_{m-1,N} \\ &= \Delta_{m,N-1} \Delta_{m,N+1} (1 - \Delta_{1,N}^2). \end{aligned} \quad (12)$$

As a consequence of these equations, one may obtain the following strong coupling  $U(N)$  results [19, 20]:

$$\Delta_{1,N}(\beta) = J_N(2N\beta) + O(\beta^{3N+2}), \quad (13)$$

$$\begin{aligned} \Delta_{2,N}(\beta) &= J_N(2N\beta)^2 - J_{N-1}(2N\beta) J_{N+1}(2N\beta) \\ &+ O(\beta^{4N}), \end{aligned} \quad (14)$$

$$\tilde{F}_N(\beta) = N^2\beta^2 - \sum_{k=1}^{\infty} kJ_{N+k}(2N\beta)^2 + O(\beta^{4N+4}) . \quad F_N(\beta) = \tilde{F}_N(\beta) + \ln \sum_{k=-\infty}^{\infty} \langle (\det U)^k \rangle , \quad (16)$$

(15)

The passage to  $SU(N)$  is effected by the relationship implying

---


$$F_N(\beta) = N^2\beta^2 + 2J_N(2N\beta) - 2J_{N-1}(2N\beta)J_{N+1}(2N\beta) - \sum_{k=1}^{\infty} kJ_{N+k}^2(2N\beta) + O(\beta^{3N}) . \quad (17)$$

We can now make use of known relationships concerning the series expansion of a product of Bessel functions to obtain a wide number of “standard” integrals:

$$S_{p,p} = p! , \quad p \leq N , \quad (18)$$

$$S_{p,N+p} = \sum_{q=0}^p (-1)^q \frac{(N+p)!}{(N+q)!} \binom{p}{q} , \quad p \leq N+1 , \quad (19)$$

$$S_{N+p,N+p} = (N+p)! + \sum_{q=1}^p \frac{(-1)^q}{(p-q)!} \left[ \frac{(N+p)!}{(N+q)!} \right]^2 \binom{2N+2q-2}{q-1} , \quad p \leq N+1 , \quad (20)$$

$$S_{p,2N+p} = \sum_{q=0}^p (-1)^q \frac{(2N+2q)!(2N+p)!}{(2N+q)!(N+q+1)!(N+q)!} \binom{p}{q} , \quad p \leq N+1 . \quad (21)$$

One may check that essentially all Hansen’s results [17] are correctly reproduced and extended to arbitrary  $N$  by the above formulas. Equations (18)–(21) are our first set of compact results concerning  $SU(N)$  integration.

Even more important is however the possibility of extracting similar results for the coefficients of the character expansion. Let us briefly recall from Ref. [18] the following expression of  $U(N)$  character coefficients  $\tilde{z}_{(r)}(\beta)$ :

$$d_{\lambda_1 \dots \lambda_N} \tilde{z}_{\lambda_1 \dots \lambda_N} = \frac{\det [I_{\lambda_i + j - i}(2N\beta)]}{\det [I_{j-i}(2N\beta)]} \equiv \langle \chi_{(r)}^*(U) \rangle . \quad (22)$$

Its  $SU(N)$  counterpart can be represented in the form

---


$$Nz_1(\beta) = \frac{\partial}{\partial(2N\beta)} F_N(\beta) = N\beta + J_{N-1}(2N\beta) - J_{N+1}(2N\beta) - \sum_{k=0}^{\infty} J_{N+k}(2N\beta)J_{N+k+1}(2N\beta) + O(\beta^{3N-1}) . \quad (26)$$

Moreover we may want to restrict our attention to the first  $\sim 2N$  orders of the strong coupling series, in order to exploit the techniques discussed in the first part of this section. In this case the character coefficients of  $U(N)$  can be reconstructed by the use of Schwinger-Dyson equations [18]. Appendix A is devoted to a presentation of our main results concerning the compact evaluation of  $U(N)$  and  $SU(N)$  character coefficients.

For what concerns the physical problem of evaluating the  $d$ -dimensional free-energy density in  $SU(N) \times SU(N)$

---


$$z_{(r)} = \frac{\sum_{s=-\infty}^{\infty} \tilde{z}_{(r+s \cdot 1^N)}}{\sum_{s=-\infty}^{\infty} \tilde{z}_{(s \cdot 1^N)}} , \quad (23)$$

where, by definition,

$$\tilde{z}_{(s \cdot 1^N)} = \langle (\det U)^s \rangle , \quad (24)$$

$$d_{(r)} \tilde{z}_{(r+s \cdot 1^N)} = \langle (\det U)^s \chi_{(r)}^*(U) \rangle , \quad (25)$$

and all quantities are computed with the  $U(N)$  measure. These results become however rapidly useless with growing  $N$ , due to the intractability of the determinants. We may however easily recover from the previous results the coefficient of the fundamental character:

---

chiral models within the strong coupling expansion, we address the reader to Ref. [18] for a discussion of the relationship between the  $SU(N)$  and the  $U(N)$  character expansions. Suffice it to say that knowing the  $U(N)$  expansion to  $O(\beta^{2m})$  allows an immediate identification with the corresponding  $SU(N)$  expansion when  $N > m$ . When  $N = m$  only a minor modification is required in order to avoid a double counting due to the self-duality of the representation  $(1^{N/2}; 0) = (0; 1^{N/2})$ . When  $N < m$  the procedure must be much more careful, but in any

case this condition would violate the already mentioned restriction on the applicability of our approach, which does not trivially extend to more than  $2N$  orders of the strong coupling series.

In order to exhibit some new results concerning the

strong coupling series for the free energy of the principal chiral models, let us first introduce the notion of “potential” intimately related to that presented by Green and Samuel in Ref. [18]:

$$W_{st} = \left[ z_{(2;0)}^s d_{(2;0)}^t + z_{(1^2;0)}^s d_{(1^2;0)}^t + 2^{1-t} z_{(1,1)}^s d_{(1,1)}^t - 2^{2-t} N^{2t} z_1^{2s} \right] N^{2-2t} . \quad (27)$$

For comparison, we mention that

$$W_{st} = V_{st} + 2^{1-t} \bar{V}_{st} , \quad (28)$$

where  $V$  and  $\bar{V}$  have been defined in Ref. [18]. The tenth order strong coupling character expansion for the free energy in  $d$  dimensions is then [21]

$$\begin{aligned} \mathcal{F} = & \binom{d}{1} \frac{F_N}{N^2} + 2 \binom{d}{2} (z_1^4 + W_{42}) + \left[ 4 \binom{d}{2} + 32 \binom{d}{3} \right] z_1^6 \\ & + \left[ 8 \binom{d}{2} + 48 \binom{d}{3} \right] \left[ \frac{1}{2} W_{11} z_1^6 + W_{31} z_1^4 \right] + \left[ 14 \binom{d}{2} + 372 \binom{d}{3} + 1296 \binom{d}{4} \right] z_1^8 \\ & + 96 \binom{d}{3} W_{21} z_1^6 + \left[ 24 \binom{d}{2} + 576 \binom{d}{3} + 1536 \binom{d}{4} \right] W_{11} z_1^8 \\ & + \left[ 56 \binom{d}{2} + 4656 \binom{d}{3} + 46272 \binom{d}{4} + 95232 \binom{d}{6} \right] z_1^{10} . \end{aligned} \quad (29)$$

Equation (29) holds for all  $U(N)$  and for  $SU(N)$  when  $N \geq 5$ . The  $SU(N)$  result for the “potential”  $W_{st}$  can be obtained in the form

$$\begin{aligned} W_{st} \simeq & \frac{\beta^{2s}}{2^t} \left[ 1 + \frac{4s}{N\beta} J'_N(2N\beta) \right] N^2 \left[ \left( 1 + \frac{1}{N} \right)^{t-s} + \left( 1 - \frac{1}{N} \right)^{t-s} + 2 \left( 1 - \frac{1}{N^2} \right)^{t-s} - 4 \right] \\ & + \beta^{2s-2} \frac{2s}{2^t} N^2 \left[ J_{N+2}(2N\beta) \left( 1 + \frac{1}{N} \right)^{t-s} + J_{N-2}(2N\beta) \left( 1 - \frac{1}{N} \right)^{t-s} - 2J_N(2N\beta) \left( 1 - \frac{1}{N^2} \right)^{t-s} \right] . \end{aligned} \quad (30)$$

By explicitly expanding in powers of  $\beta$  the 14th order character expansion for the free energy [presented in Ref. [18] up to  $O(\beta^{12})$ ], we obtain, for  $U(N)$  models ( $N \geq 7$ ),

$$\begin{aligned} \tilde{\mathcal{F}} = & 2\beta^2 + 2\beta^4 + 4\beta^6 + \left[ 14 + \frac{N^2(5N^2 - 2)}{(N^2 - 1)^2} \right] \beta^8 + \left[ 56 + \frac{8N^2(5N^2 - 2)}{(N^2 - 1)^2} \right] \beta^{10} \\ & + \left[ 248 + \frac{8N^2(35N^2 - 17)}{(N^2 - 1)^2} + \frac{2N^2(14N^6 - 11N^4 + 8N^2 - 2)}{(N^2 - 1)^4} + \frac{16N^4(9N^4 - 26N^2 + 8)}{3(N^2 - 1)^2(N^2 - 4)^2} \right] \beta^{12} \\ & + \left[ 1176 + \frac{432N^2}{N^2 - 1} - \frac{32N^4}{(N^2 - 1)^2} + \frac{240N^2(5N^2 - 2)}{(N^2 - 1)^2} + \frac{N^2(248N^4 - 144N^2 + 48)}{(N^2 - 1)^3} \right. \\ & \left. + \frac{N^2(436N^6 - 344N^4 + 208N^2 - 48)}{(N^2 - 1)^4} + \frac{64N^4(9N^4 - 26N^2 + 8)}{(N^2 - 1)^2(N^2 - 4)^2} \right] \beta^{14} + O(\beta^{16}) , \end{aligned} \quad (31)$$

and, for the  $SU(N)$  models ( $N \geq 7$ ),

$$\begin{aligned} \mathcal{F} = & \tilde{\mathcal{F}} + \frac{4N^{N-2}}{N!} \beta^N + \left[ -\frac{4N^N}{(N+1)!} + \frac{8N^{N-1}}{N!} \right] \beta^{N+2} \\ & + \left[ \frac{2N^{N+2}}{(N+2)!} - \frac{8(N+2)N^N}{(N+1)!} + \frac{4N^{N+1}}{(N-1)N!} + \frac{24N^{N-1}}{N!} + \frac{4N^{N-2}}{(N-2)!} \right] \beta^{N+4} \\ & + \left[ -\frac{2N^{N+4}}{3(N+3)!} + \frac{4N^{N+2}(N+4)}{(N+2)!} - \frac{4N^{N+1}(N^2+4N+2)}{(N+1)(N+1)!} + \frac{8N^{N+1}(1+N-N^2)}{(N^2-1)(N+1)!} \right. \\ & + \frac{4N^{N+3}}{3(N-1)(N-2)N!} - \frac{24N^N(N+2)}{(N+1)!} - \frac{4N^N}{(N-1)!} - \frac{8N^N}{N!} + \frac{24N^{N+1}}{(N-1)N!} \\ & \left. + \frac{4N^N}{(N-1)^2(N-3)!} + \frac{112N^{N-1}}{N!} + \frac{24N^{N-2}}{(N-2)!} \right] \beta^{N+6} + O(\beta^{N+8}) . \end{aligned} \quad (32)$$

The  $SU(6)$  result, including an analysis of the  $O(\beta^{2N})$  contribution, is finally

$$\mathcal{F} = 2\beta^2 + 2\beta^4 + \frac{56}{5}\beta^6 + \frac{84\,038}{1225}\beta^8 + \frac{459\,308}{1225}\beta^{10} + \frac{548\,436\,429}{85\,750}\beta^{12} + \dots \quad (33)$$

The strong coupling series of the internal energy  $E$  can be obtained by

$$E = 1 - \frac{1}{4} \frac{d\mathcal{F}}{d\beta} \quad (34)$$

In order to extend the strong coupling series of thermodynamical functions to higher orders and in order to compute the strong coupling series of correlation functions, it will prove convenient to define more involved potentials corresponding to nontrivial loop topologies and three-body interactions. For the purposes of the present paper, and in view of further developments, we shall define

$$\widetilde{W}_{ab} = z_{(1;1)}^{a+b} + N^2 \left[ z_{(1;1)}^a \frac{d_{(1;1)}}{4} \left( \frac{z_{(2;0)}^b}{d_{(2;0)}} + \frac{z_{(1^2;0)}^b}{d_{(1^2;0)}} \right) + z_{(1;1)}^b \frac{d_{(1;1)}}{4} \left( \frac{z_{(2;0)}^a}{d_{(2;0)}} + \frac{z_{(1^2;0)}^a}{d_{(1^2;0)}} \right) - 2z_1^{2a+2b} \right], \quad (35)$$

$$\begin{aligned} W_{abc} &= z_{(1;1)}^a \left( z_{(2;0)}^b d_{(2;0)} + z_{(1^2;0)}^b d_{(1^2;0)} \right) \left( z_{(2;0)}^c d_{(2;0)} + z_{(1^2;0)}^c d_{(1^2;0)} \right) - 2N^2 W_{a1} z_1^{2b+2c} \\ &\quad - z_{(1;1)}^a \left( z_{(2;0)}^{b+c} d_{(2;0)} + z_{(1^2;0)}^{b+c} d_{(1^2;0)} \right) + \text{permutations of } (a, b, c) \\ &\quad + z_{(1;1)}^{a+b+c} \left( d_{(1;1)}^2 - d_{(1;1)} \right) - 4N^4 z_1^{2a+2b+2c}, \end{aligned} \quad (36)$$

and the three-body potentials

$$\begin{aligned} V_{qst} &= N^{1-2t} \left[ \left( z_{(3;0)}^q d_{(3;0)} + z_{(2,1;0)}^q d_{(2,1;0)} + z_{(2,1)}^q d_{(2,1)} \right) z_{(2;0)}^s d_{(2;0)}^t \right. \\ &\quad + \left( z_{(2,1;0)}^q d_{(2,1;0)} + z_{(1^3;0)}^q d_{(1^3;0)} + z_{(1^2,1)}^q d_{(1^2,1)} \right) z_{(1^2;0)}^s d_{(1^2;0)}^t \\ &\quad + 2^{1-t} \left( z_{(2;1)}^q d_{(2;1)} + z_{(1^2,1)}^q d_{(1^2,1)} \right) z_{(1;1)}^s d_{(1;1)}^t - 2N^{2t+1} z_1^q W_{q+s,t+1} \\ &\quad \left. - 2^{2-t} N^{2t+1} z_1^{q+2s} W_{q,1} - 2^{2-t} N^{2t+3} z_1^{3q+2s} \right]. \end{aligned} \quad (37)$$

### III. STRONG COUPLING EXPANSION OF CORRELATION FUNCTIONS

A typical application of the strong coupling analysis amounts to the evaluation of the so-called “true mass gap” of the model, which in turn is defined to be the coefficient of the asymptotic exponential decay of the two point correlation function of the order parameter. In  $SU(N) \times SU(N)$  chiral models one defines

$$G(x) = \frac{1}{N} \langle \text{Tr} [U^\dagger(x)U(0)] \rangle \quad (38)$$

and the true mass gap is

$$\mu = - \lim_{|x| \rightarrow \infty} \frac{\ln G(x)}{|x|} \quad (39)$$

It is also possible to introduce the lattice momentum transform

$$\widetilde{G}(p) = \sum_x G(x) \exp \left( i \frac{2\pi p \cdot x}{L} \right) \quad (40)$$

and extract the mass gap from the (imaginary momentum) pole singularity of  $\widetilde{G}(p)$ , i.e., by solving the equation

$$\widetilde{G}^{-1}(p = i\mu) = 0 \quad (41)$$

There are a few well-known (but not necessarily well understood) results concerning the evaluation of the mass

gap. In particular it is often stated that in the strong coupling regime  $G(x)$  “does not exponentiate” and it is therefore necessary to define the wall-wall correlation

$$G_w(x_{\parallel}) = \sum_{x_{\perp}} G(x_{\perp}, x_{\parallel}) \quad (42)$$

enjoying the exponentiation property, and assume

$$\mu = - \lim_{|x_{\parallel}| \rightarrow \infty} \frac{\ln G_w(x_{\parallel})}{|x_{\parallel}|} \quad (43)$$

Appendix B is devoted to a short discussion of this question, which finds an easy illustration in the context of the exactly solvable Gaussian model.

In practice, when extracting physical quantities from Monte Carlo simulations, one typically faces a situation where it is nonrealistic to solve numerically Eq. (41), which requires an analytic continuation to negative  $p^2$  of the (usually poorly known) function  $\widetilde{G}^{-1}(p)$ . We shall be able to perform this exercise in our specific study, but this is far from being an easily generalizable practice. On the other side, working on a finite lattice often prevents us from exploring a sizable region where exponentiation may hold with small errors for arbitrary  $\beta$ . We therefore found it convenient to analyze explicitly the strong coupling expansion of the Green’s function  $G(x)$  for finite fixed lattice distance in order to establish a benchmark

both for exponentiation and for the analysis of the numerical results.

Without entering many details of the (sometimes cumbersome) strong coupling calculations, we want to sketch the main ingredients and logical steps before presenting our results. In passing we notice that we might consider a slightly more general Green’s function than Eq. (38):

$$G_{(r)} = \frac{\langle \chi_{(r)} [U^\dagger(x)U(0)] \rangle}{d_{(r)}} \quad (44)$$

where  $r$  can be restricted, for principal chiral models, to the completely antisymmetric representations  $(1^n; 0)$ . The strong coupling expansion is naturally ordered in the length of the path that we choose in order to connect the

point  $x = (x_1, x_2)$  with the origin. In turn, since every path can be decomposed into a sum of shorter paths, we may in general establish recursive relationships connecting the (fixed length) contributions to  $G(x_1, x_2)$  with the (shorter length) contributions to Green’s functions of nearby points.

The strong coupling character expansion of Green’s functions involves, to lowest orders, only a summation over properly weighted self-avoiding walks. The effect of “potentials” is a higher order contribution that must be included by considering bifurcating paths “dressed” with properly chosen representations of the link operators. For all  $U(N)$  groups ( $N \geq 2$ ) and  $SU(N)$  groups ( $N \geq 4$ ) the  $O(\beta^5)$  strong coupling character expansion may be represented by

---


$$G(x_1, x_2) = z_1^{x_1+x_2} \left[ C_0(x_1, x_2) + C_2(x_1, x_2)z_1^2 + C_4(x_1, x_2)z_1^4 + A(x_1, x_2)z_1^2 W_{11} + B(x_1, x_2) W_{21} + O(z_1^6) \right] \quad (45)$$

where the quantities  $C_{2k}(x_1, x_2)$  represent the number of self-avoiding walks connecting the origin with the lattice point  $x = (x_1, x_2)$  and whose length is  $l = x_1 + x_2 + 2k$ , while the functions  $A$  and  $B$  satisfy the relationship

$$A(x_1, x_2) + 2B(x_1, x_2) = 2(x_1 + x_2) C_0(x_1, x_2) \quad (46)$$

In Appendix C we derived the results

$$C_0(x_1, x_2) = \binom{x_1 + x_2}{x_1} \equiv \binom{x_1 + x_2}{x_2} \quad (47)$$

$$C_2(x_1, x_2) = \binom{x_1 + x_2}{x_1} \left[ \frac{x_1(x_1 + 1)}{x_2 + 1} + \frac{x_2(x_2 + 1)}{x_1 + 1} \right] \quad (48)$$

$$C_4(x_1, x_2) = \binom{x_1 + x_2}{x_1} \left[ x_1 x_2 + 2x_1 + 2x_2 + \frac{x_2(x_2 + 3)}{x_1 + 1} + \frac{x_1(x_1 + 3)}{x_2 + 1} + \frac{(x_2 - 1)x_2(x_2 + 1)(x_2 + 2)}{2(x_1 + 1)(x_1 + 2)} + \frac{(x_1 - 1)x_1(x_1 + 1)(x_1 + 2)}{2(x_2 + 1)(x_2 + 2)} - \frac{2x_1 x_2}{x_1 + x_2} \right] \quad (49)$$

$$A(x_1, x_2) = 2 \frac{x_1^2 + x_2^2}{x_1 + x_2} C_0(x_1, x_2) \quad (50)$$

$$B(x_1, x_2) = \frac{2x_1 x_2}{x_1 + x_2} C_0(x_1, x_2) \quad (51)$$

Writing down and solving recursion equations for the coefficients of the strong coupling series for Green’s functions is a very powerful but by no means simple or efficient approach to the evaluation of the mass gap. In practice we may observe that, to any given order of the strong coupling expansion, the recursive relations between coefficients imply that only a finite number of short distance wall-wall correlations for  $L \leq \bar{L}$  may violate exact exponentiation because of boundary condition effects. Therefore one may compute the quantities

$$\ln G_w(L + 1) - \ln G_w(L) \quad (52)$$

for the first few values of  $L$  until they become constant. The constants obtained are directly related to the masses by the relationships

---


$$\mu_{\text{side}} = \ln G_{\text{side}}(L) - \ln G_{\text{side}}(L + 1) \quad , \quad L > \bar{L}_s \quad (53)$$

$$\frac{\mu_{\text{diag}}}{\sqrt{2}} = \ln G_{\text{diag}}(L) - \ln G_{\text{diag}}(L + 1) \quad , \quad L > \bar{L}_d \quad (54)$$

where by definition

$$G_{\text{side}}(L) \equiv \sum_{x_2=-\infty}^{\infty} G(L, x_2) \quad , \quad (55)$$

$$G_{\text{diag}}(L) \equiv \sum_{x_2=-\infty}^{\infty} G(L - x_2, x_2) \quad . \quad (56)$$

It is possible to prove that the alternative definition of  $\mu$  based on solving the equation

$$\tilde{G}^{-1}(p = i\mu) = 0 \quad (57)$$

perturbatively in the strong coupling expansion parameter gives stable results only after all correlations up to  $L = \bar{L}$  have been included in the Fourier transform of the propagator, and the result obviously coincides with Eqs. (53) and (54). It is therefore convenient to construct explicitly the Fourier transform of the inverse propagator and extract the relevant physical parameters by a direct analysis of this last quantity, making use of the above considerations in order to establish the accuracy of the computations, which in general will not coincide with the precision reached in the evaluation of  $\tilde{G}^{-1}(p)$ .

The evaluation of  $\tilde{G}^{-1}(p)$  is dramatically simplified by the observation that any strong coupling expanded two-point Green's function can be unambiguously separated into the form

$$G(x) = G_0(x) + \Delta G(x) , \quad (58)$$

where  $G_0(x)$  is originated by the Fourier transform of the generalized Gaussian propagator

$$\tilde{G}_0(p) = \frac{1}{A_0(z_1) - 2z_1 B_0(z_1) \sum_{\mu} \cos p_{\mu}} , \quad (59)$$

and the functions  $A_0(z_1)$  and  $B_0(z_1)$  are uniquely determined by the conditions

$$\begin{aligned} G_0(0) &= 1 , \\ G_0(1, 0) &= 1 - E(z_1) = \frac{1}{4} \frac{d\mathcal{F}}{d\beta} \equiv \varepsilon(z_1) , \end{aligned} \quad (60)$$

which can be cast into the form

$$\begin{aligned} 1 &= \frac{1}{A_0} \sum_{n=0}^{\infty} \binom{2n}{n} \left( \frac{zB_0}{A_0} \right)^{2n} , \\ zB_0 &= \frac{A_0 - 1}{4\varepsilon} . \end{aligned} \quad (61)$$

From the results of the previous section we may extract

$$\begin{aligned} \varepsilon(z_1) &= z_1 + 2z_1^3 + 6z_1^5 + 2z_1^3 W_{11} + 28z_1^7 + 12z_1^5 W_{11} + 2z_1 W_{31} \\ &\quad + 140z_1^9 + 76z_1^7 W_{11} + 6z_1^5 W_{20} + 8z_1^3 W_{31} + 2V_{131} + z_1^6 V_{100} + O(z_1^{11}) . \end{aligned} \quad (62)$$

As a consequence we obtain

$$\begin{aligned} A_0(z_1) &= 1 + 4z_1^2 + 12z_1^4 + 60z_1^6 + 16z_1^4 W_{11} + 316z_1^8 + 96z_1^6 W_{11} + 16z_1^2 W_{31} + 1844z_1^{10} \\ &\quad + 848z_1^8 W_{11} + 64z_1^6 W_{11}^2 + 48z_1^6 W_{20} + 64z_1^4 W_{31} + 16z_1 V_{131} + 8z_1^7 V_{100} + O(z_1^{12}) , \end{aligned} \quad (63)$$

$$\begin{aligned} B_0(z_1) &= 1 + z_1^2 + 7z_1^4 + 2z_1^2 W_{11} + 31z_1^6 + 6z_1^4 W_{11} + 2z_1^2 W_{31} + 189z_1^8 + 86z_1^6 W_{11} \\ &\quad + 6z_1^4 W_{11}^2 + 6z_1^4 W_{20} + 2z_1^2 W_{31} + 2z_1^{-1} V_{131} + z_1^5 V_{100} + O(z_1^{10}) . \end{aligned} \quad (64)$$

A direct evaluation of all coordinate-space Green's functions that are nontrivial to  $O(z_1^{10})$  allows us to determine  $\Delta G(x)$  with the same precision, since  $G_0(x)$  is easily obtained by antitransforming Eq. (59). By noticing that the first nontrivial contributions to  $\Delta G(x)$  are  $O(z_1^6)$ , it is now relatively easy to evaluate directly  $\tilde{G}^{-1}(p)$  to  $O(z_1^{10})$ . We obtained

$$\tilde{G}^{-1}(p) = A(z_1) + z_1 B(z_1) \hat{p}^2 + z_1^6 C(z_1) \hat{p}_1^2 \hat{p}_2^2 + z_1^8 D(z_1) (\hat{p}_1^4 + \hat{p}_2^4) + z_1^9 E(z_1) \hat{p}^2 \hat{p}_1^2 \hat{p}_2^2 + O(z_1^{11}) , \quad (65)$$

where  $\hat{p}_{\mu}^2 = 4 \sin^2(p_{\mu}/2)$ ,  $\hat{p}^2 = \sum_{\mu} \hat{p}_{\mu}^2$ , and

$$\begin{aligned} A(z_1) &= A_0(z_1) - 4z_1 B_0(z_1) - 8\Delta^{(1)} z_1^6 (1 - 4z_1 + 3z_1^2 + 6z_1^3 - 3z_1^4) \\ &\quad - 16\Delta^{(2)} z_1^8 (1 - 4z_1 + 2z_1^2) - 8\Delta^{(3)} z_1^9 - 8\Delta^{(4)} z_1^{10} - 16\Delta^{(5)} z_1^{10} + O(z_1^{11}) , \end{aligned} \quad (66)$$

$$\begin{aligned} B(z_1) &= B_0(z_1) + 4\Delta^{(1)} z_1^5 (1 - 2z_1 + 2z_1^2 + 3z_1^3) + 8\Delta^{(2)} z_1^7 (1 - 2z_1) + 10\Delta^{(3)} z_1^8 + 8\Delta^{(4)} z_1^9 + 8\Delta^{(5)} z_1^9 + O(z_1^{10}) , \end{aligned} \quad (67)$$

$$C(z_1) = -2\Delta^{(1)} - 4\Delta^{(2)} z_1^2 - 8\Delta^{(3)} z_1^3 - 4\Delta^{(5)} z_1^4 + O(z_1^5) , \quad (68)$$

$$D(z_1) = -2\Delta^{(1)} - 2\Delta^{(3)} z_1 - 2\Delta^{(4)} z_1^2 + O(z_1^3) , \quad (69)$$

$$E(z_1) = \Delta^{(3)} + O(z_1^2) . \quad (70)$$

We have defined the following combinations of potentials:

$$\Delta^{(1)} = z_1^{-4}W_{21} - 2z_1^{-2}W_{11} - 1, \quad (71)$$

$$\Delta^{(2)} = -z_1^{-6}W_{31} + 4z_1^{-4}W_{21} + z_1^{-2}W_{10} - 7z_1^{-2}W_{11} - 4, \quad (72)$$

$$\Delta^{(3)} = z_1^{-2}\widetilde{W}_{11} + 2z_1^{-6}W_{31} - 4z_1^{-4}W_{21} - 2z_1^{-2}W_{10} + 4z_1^{-2}W_{11} + 1, \quad (73)$$

$$\Delta^{(4)} = 2z_1^{-6}\widetilde{W}_{21} + z_1^{-6}W_{111} - 2z_1^{-4}\widetilde{W}_{11} - 4z_1^{-6}W_{31} + z_1^{-8}W_{41} + 16z_1^{-4}W_{21} \\ - 2z_1^{-4}W_{20} - 3z_1^{-4}W_{11}^2 - 26z_1^{-2}W_{11} + 4z_1^{-2}W_{10} - 9, \quad (74)$$

$$\Delta^{(5)} = z_1^{-5}V_{110} + \frac{1}{2}z_1^{-10}V_{221} - z_1^{-9}V_{131} - z_1^{-3}V_{100} - z_1^{-4}\widetilde{W}_{11} + z_1^{-8}W_{41} - 8z_1^{-6}W_{31} \\ + \frac{55}{2}z_1^{-4}W_{21} - 3z_1^{-4}W_{20} - \frac{9}{2}z_1^{-4}W_{11}^2 - 53z_1^{-2}W_{11} + 13z_1^{-2}W_{10} + z_1W_{11}W_{21} + \frac{1}{2}W_{0,-1} - \frac{53}{2}. \quad (75)$$

Equation (65) is a rather compact collection of physically relevant results concerning the strong coupling regime of the models under investigations. We notice that the nearest-neighbor Gaussian structure of the propagator starts being violated to  $O(z_1^6)$  in diagonal correlations and only to  $O(z_1^8)$  in side correlations. We therefore expect a substantial agreement of the ratio  $\xi_G/\xi_w$ , where  $\xi_G^2 \equiv \langle x^2 \rangle$  and  $\xi_w \equiv 1/\mu_{\text{side}}$ , with its Gaussian value even for not too strong values of the coupling (as we will see in Sec. V).

By standard arguments we can establish relationships between the propagator, the susceptibility and its second moment:

$$\chi = \sum_{x_1, x_2} G(x_1, x_2) = G_{\text{side}}(0) + 2 \sum_{L=1}^{\infty} G_{\text{side}}(L) \\ = G_{\text{diag}}(0) + 2 \sum_{L=1}^{\infty} G_{\text{diag}}(L) = \frac{1}{A(z_1)}, \quad (76)$$

$$\chi(x^2) = \frac{1}{4} \sum_{x_1, x_2} (x_1^2 + x_2^2) G(x_1, x_2) = \sum_{L=1}^{\infty} L^2 G_{\text{side}}(L) \\ = \frac{1}{2} \sum_{L=1}^{\infty} L^2 G_{\text{diag}}(L) = \frac{z_1 B(z_1)}{A(z_1)^2}. \quad (77)$$

Hence we obtain

$$M_G^2 \equiv \frac{1}{\langle x^2 \rangle} = \frac{A(z_1)}{z_1 B(z_1)}, \quad (78)$$

$$Z_G = \frac{1}{z_1 B(z_1)}. \quad (79)$$

Moreover, by solving appropriate algebraic equations we find

$$M_{\text{side}}^2 = 2 (\cosh \mu_{\text{side}} - 1) \simeq M_G^2 + \frac{z_1^5 A(z_1)^2 D(z_1)}{B(z_1)^3} + \dots, \quad (80)$$

$$M_{\text{diag}}^2 = 4 \left( \cosh \frac{\mu_{\text{diag}}}{\sqrt{2}} - 1 \right) \simeq M_G^2 + \frac{A(z_1)^2}{B(z_1)^3} \left( \frac{z_1^5 D(z_1)}{2} + \frac{z_1^3 C(z_1)}{4} \right) - \frac{z_1^5 A(z_1)^3 E(z_1)}{4B(z_1)^4} + \dots. \quad (81)$$

By substituting our explicit results we find

$$\chi = 1 + 4z_1 + 12z_1^2 + 36z_1^3 + 100z_1^4 + (284 + 8z_1^{-2}W_{11})z_1^5 + (788 + 48z_1^{-2}W_{11} + 8\Delta^{(1)})z_1^6 \\ + (2204 + 216z_1^{-2}W_{11} + 8z_1^{-6}W_{31} + 32\Delta^{(1)})z_1^7 + (6068 + 800z_1^{-2}W_{11} + 48z_1^{-6}W_{31} + 88\Delta^{(1)} \\ + 16\Delta^{(2)})z_1^8 + (16820 + 8z_1^{-9}V_{131} + 4z_1^{-4}V_{100} + 2904z_1^{-2}W_{11} + 24z_1^{-4}W_{11}^2 + 24z_1^{-4}W_{20} \\ + 200z_1^{-6}W_{31} + 304\Delta^{(1)} + 64\Delta^{(2)} + 8\Delta^{(3)})z_1^9 + (46172 + 48z_1^{-9}V_{131} + 24z_1^{-4}V_{100} + 9840z_1^{-2}W_{11} \\ + 192z_1^{-4}W_{11}^2 + 144z_1^{-4}W_{20} + 704z_1^{-6}W_{31} + 1000\Delta^{(1)} + 160\Delta^{(2)} + 64\Delta^{(3)} + 8\Delta^{(4)} + 16\Delta^{(5)})z_1^{10} + O(z_1^{11}), \quad (82)$$

$$\begin{aligned}
z_1 M_G^2 = & 1 - 4z_1 + 3z_1^2 + \left(2 - 2z_1^{-2}W_{11}\right)z_1^4 - 4\Delta^{(1)}z_1^5 + \left(6 + 6z_1^{-2}W_{11} - 2z_1^{-6}W_{31} + 16\Delta^{(1)}\right)z_1^6 \\
& - \left(16\Delta^{(1)} + 8\Delta^{(2)}\right)z_1^7 + \left(14 - 2z_1^{-9}V_{131} - z_1^{-4}V_{100} - 4z_1^{-2}W_{11} - 2z_1^{-4}W_{11}^2 - 6z_1^{-4}W_{20}\right. \\
& + 10z_1^{-6}W_{31} + 4\Delta^{(1)} + 32\Delta^{(2)} - 10\Delta^{(3)}\left.)z_1^8 + \left(12\Delta^{(1)} - 16\Delta^{(2)} + 32\Delta^{(3)} - 8\Delta^{(4)}\right. \right. \\
& \left. \left. - 8\Delta^{(5)} + 16z_1^{-2}W_{11}\Delta^{(1)}\right)z_1^9 + O(z_1^{10}) , \tag{83}
\end{aligned}$$

$$\begin{aligned}
z_1 Z_G = & 1 - z_1^2 + \left(-6 - 2z_1^{-2}W_{11}\right)z_1^4 - 4\Delta^{(1)}z_1^5 + \left(-18 - 2z_1^{-2}W_{11} - 2z_1^{-6}W_{31} + 8\Delta^{(1)}\right)z_1^6 \\
& - 8\Delta^{(2)}z_1^7 + \left(-98 - 2z_1^{-9}V_{131} - z_1^{-4}V_{100} - 52z_1^{-2}W_{11} - 2z_1^{-4}W_{11}^2 - 6z_1^{-4}W_{20} + 2z_1^{-6}W_{31}\right. \\
& \left. - 28\Delta^{(1)} + 16\Delta^{(2)} - 10\Delta^{(3)}\right)z_1^8 + \left(60\Delta^{(1)} + 16\Delta^{(2)} - 8\Delta^{(4)} - 8\Delta^{(5)} + 16z_1^{-2}W_{11}\Delta^{(1)}\right)z_1^9 + O(z_1^{10}) , \tag{84}
\end{aligned}$$

$$\begin{aligned}
\mu_{\text{side}} = & -\ln z_1 - 2z_1 - \left(2 + 2z_1^{-2}W_{11}\right)z_1^4 - \left(\frac{22}{5} + 4z_1^{-2}W_{11} + 4\Delta^{(1)}\right)z_1^5 \\
& - \left(4 + 2z_1^{-6}W_{31} - 6\Delta^{(1)}\right)z_1^6 - \left(\frac{86}{7} + 4z_1^{-2}W_{11} + 4z_1^{-6}W_{31} - 16\Delta^{(1)} + 8\Delta^{(2)} + 2\Delta^{(3)}\right)z_1^7 \\
& - \left(28 + 32z_1^{-2}W_{11} + 4z_1^{-4}W_{11}^2 + 6z_1^{-4}W_{20} - 4z_1^{-6}W_{31} + 2z_1^{-9}V_{131} + z_1^{-4}V_{100} + 28\Delta^{(1)}\right. \\
& \left. - 16\Delta^{(2)} - 2\Delta^{(3)} + 2\Delta^{(4)}\right)z_1^8 - 2\Delta^{(6)}z_1^8 + O(z_1^9) , \tag{85}
\end{aligned}$$

$$\begin{aligned}
\frac{\mu_{\text{diag}}}{\sqrt{2}} = & -\ln 2z_1 - z_1^2 - \left(\frac{5}{2} + 2z_1^{-2}W_{11} + \frac{1}{2}\Delta^{(1)}\right)z_1^4 \\
& - \left(\frac{25}{3} + 4z_1^{-2}W_{11} + 2z_1^{-6}W_{31} - 2\Delta^{(1)} + \Delta^{(2)} + \frac{1}{4}\Delta^{(3)}\right)z_1^6 + O(z_1^7) . \tag{86}
\end{aligned}$$

The contribution proportional to

$$\Delta^{(6)} \equiv z_1^{-6}W_{31} - 2z_1^4W_{21} + z_1^2W_{11} \tag{87}$$

in Eq. (85) was obtained by evaluating the  $O(z_1^{11})$  contribution to  $G(3,0)$  and could not have been predicted from the knowledge of the  $O(z_1^{10})$  contributions to  $\tilde{G}^{-1}(p)$ : This is in accord with our previously discussed considerations. Further useful results are

$$\begin{aligned}
\ln G_{\text{side}}(L) = & L \ln z_1 + 2(L+1)z_1 + \frac{2}{3}(L+7)z_1^3 + 2(L+2)z_1^4 + \frac{2}{5}(L+51)z_1^5 + 2Lz_1^2W_{11} \\
& - 4(L-1)z_1^3W_{11} + 4Lz_1W_{21} + 2(5L+9)z_1^6 + 4(3L+1)z_1^4W_{11} - 2(3L+1)z_1^2W_{21} + 2LW_{31} \\
& + 2z_1^6\Delta^{(1)}\delta_{L,0} + \frac{4}{7}(172-3L)z_1^7 + 4(L+1)z_1^5W_{10} - 12(L-1)z_1^5W_{11} + 4(2L+3)z_1^3W_{21} \\
& + 2(L-1)z_1^3\tilde{W}_{11} + 2z_1^7\left(\Delta^{(3)} - 2\Delta^{(1)}\right)\delta_{L,0} + 22(2L+5)z_1^8 - 4(L+4)z_1^6W_{10} + 2(15L+28)z_1^6W_{11} \\
& - 2(L-3)z_1^4W_{11}^2 + 2(L+2)z_1^4W_{20} - 20z_1^4W_{21} + 2(L+6)z_1^2W_{31} + 2(L-1)W_{41} - 2(2L-3)z_1^4\tilde{W}_{11} \\
& + 4(L-1)z_1^2\tilde{W}_{21} + 2(L-1)z_1^2W_{111} + 2z_1^{-1}LV_{31} + z_1^5LV_{100} + 2z_1^8\Delta^{(6)}\delta_{L,1} \\
& + 2z_1^8\left(2\Delta^{(6)} + \Delta^{(4)} - 2\Delta^{(3)}\right)\delta_{L,0} + O(z_1^9) , \tag{88}
\end{aligned}$$

$$\begin{aligned}
\ln G_{\text{diag}}(L) = & L \ln 2z_1 + (L+4)z_1^2 + (2L + \frac{25}{2})z_1^4 + (L+1)z_1^2W_{11} + \frac{1}{2}(L-1)W_{21} \\
& + \frac{1}{2}z_1^4\Delta^{(1)}\delta_{L,0} + \frac{754+79L}{12}z_1^6 + \frac{L}{2}z_1^4W_{10} + (2L+9)z_1^4W_{11} + (L+4)z_1^2W_{21} + \frac{3}{2}LW_{31} \\
& + \frac{L-2}{4}z_1^2\tilde{W}_{11} + \frac{1}{4}z_1^6\Delta^{(3)}\delta_{L,1} + \frac{1}{2}z_1^6\left(\Delta^{(3)} + 2\Delta^{(2)} - 4\Delta^{(1)}\right)\delta_{L,0} + O(z_1^8) . \tag{89}
\end{aligned}$$

The results we have obtained are expressed in the language of the character expansion. However, within the precision of our expansion it is possible, for all  $U(N)$  and  $SU(N)$  groups with  $N$  sufficiently large, to convert the results into a standard strong coupling series by the replacements (dictated by our previous analysis)

$$z_1 \simeq \beta , \quad (90)$$

$$z_1^{-2} W_{11} \simeq 0 , \quad (91)$$

$$\frac{1}{2} W_{0,-1} \simeq z_1^{-2} W_{10} \simeq 2z_1^{-4} W_{21} \simeq \frac{4N^2}{N^2-1} \xrightarrow{N \rightarrow \infty} 4 , \quad (92)$$

$$z_1^{-4} W_{20} \simeq 2z_1^{-6} W_{31} \simeq \frac{2N^2(5N^2-2)}{(N^2-1)^2} \xrightarrow{N \rightarrow \infty} 10 , \quad (93)$$

$$z_1^{-8} W_{41} \simeq \frac{N^2(9N^4-6N^2+2)}{(N^2-1)^3} \xrightarrow{N \rightarrow \infty} 9 , \quad (94)$$

$$z_1^{-4} \widetilde{W}_{11} \simeq \frac{N^2(7N^2-2)}{(N^2-1)^2} \xrightarrow{N \rightarrow \infty} 7 , \quad (95)$$

$$z_1^{-6} \widetilde{W}_{21} \simeq \frac{N^2(11N^4-6N^2+2)}{(N^2-1)^3} \xrightarrow{N \rightarrow \infty} 11 , \quad (96)$$

$$z_1^{-6} W_{111} \simeq \frac{-4N^4}{(N^2-1)^2} \xrightarrow{N \rightarrow \infty} -4 , \quad (97)$$

$$z_1^{-4} V_{100} \simeq 0 , \quad (98)$$

$$z_1^{-5} V_{110} \simeq 0 , \quad (99)$$

$$z_1^{-9} V_{131} \simeq 0 , \quad (100)$$

$$z_1^{-10} V_{221} \simeq \frac{8N^4(3N^2-2)}{(N^2-1)^2(N^2-4)} \xrightarrow{N \rightarrow \infty} 24 . \quad (101)$$

In Appendix D we give explicitly the  $N = \infty$  strong coupling series of some relevant quantities considered in this section.

#### IV. WEAK COUPLING EXPANSION

For both continuum and lattice, at low temperature, the perturbative expansion is performed by setting

$$U = e^{iA} , \quad A = \sum_a T_a A_a \quad (102)$$

[ $T_a$  are the generators of the  $SU(N)$  group and  $A_a$  are  $N^2-1$  real fields] and expanding  $U$  in powers of  $A$ . The above change of variables introduces an additional ill-defined determinant in the partition function: Indeed [24],

$$[dU] = K \prod_a [dA_a] e^{-S_m} ,$$

$$S_m = -\frac{1}{2} \sum_n \text{Tr} \ln \frac{2(1 - \cos \tilde{A}_n)}{\tilde{A}_n^2} , \quad (103)$$

where  $\tilde{A}_{bc} = \sum_a i f_{bac} A_a$  and  $K$  is an irrelevant constant. In dimensional regularization, the measure term does not contribute, as a consequence of the rule  $\int d^d k = 0 \Leftrightarrow \delta^d(0) = 0$ , where  $d$  is the space dimension.

Short weak coupling series for the free-energy density of  $U(N)$  and  $SU(N)$  chiral models on the lattice were presented in Ref. [25]. We calculated the energy density up to three loops finding

$$E = 1 - \left\langle \frac{1}{N} \text{Re Tr} [U_n U_{n+\mu}^\dagger] \right\rangle = \frac{N^2-1}{8N^2\beta} \left[ 1 + \frac{a_1}{\beta} + \frac{a_2}{\beta^2} + \dots \right] , \quad (104)$$

where

$$a_1 = \frac{N^2-2}{32N^2} ,$$

$$a_2 = \frac{3N^4-14N^2+20}{768N^4} + \frac{N^4-4N^2+12}{64N^4} Q_1 + \frac{N^4-8N^2+24}{64N^4} Q_2 , \quad (105)$$

$Q_1$  and  $Q_2$  being numerical constants:

$$Q_1 = \int \frac{d^2 k}{(2\pi)^2} \left[ \int \frac{d^2 p}{(2\pi)^2} \left( \frac{\widehat{k}^2}{\widehat{p}^2 \widehat{p} + \widehat{k}^2} - \frac{2}{\widehat{p}^2} \right) \right]^2 ,$$

$$Q_2 = \sum_{\mu, \nu} \left[ \int \delta \left( \sum_1^4 k_i \right) \frac{(k_1 + k_2)_\mu (k_1 + k_3)_\nu}{\widehat{k}_1^2 \widehat{k}_2^2 \widehat{k}_3^2 \widehat{k}_4^2} \right] - 2 \left[ \int \frac{1}{\widehat{k}^2} \right]^2 . \quad (106)$$

$Q_1 = 0.0958876$  and  $Q_2 = -0.0670$ .

We calculated

$$G(T, x) = \frac{\int [dU] \frac{1}{N} \text{Re Tr} [U(0)U(x)^\dagger] \exp(-S/T)}{\int [dU] \exp(-S/T)} \quad (107)$$

in perturbation theory, and in two regularization schemes: dimensional and lattice regularizations. In dimensional regularization and in  $x$  space,

$$G_D(T, x, \epsilon) = 1 + \frac{N^2 - 1}{2N} \frac{T}{(2\pi)^d S_d} \frac{1}{\epsilon x^\epsilon} + \frac{N^2 - 1}{2N} \frac{N^2 - 2}{8N} \frac{T^2}{(2\pi)^{2d} S_d^2} \frac{1}{\epsilon^2 x^{2\epsilon}} + \dots, \quad (108)$$

where  $S_d = [(2\pi)^{d/2} 2^{\epsilon/2} \Gamma(1 + \epsilon/2)]^{-1}$  and  $\epsilon = d - 2$ . In  $p$  space,

$$\tilde{G}_D(T, p, \epsilon) = \frac{N^2 - 1}{2N} \frac{T}{p^2} \left[ 1 + \frac{N^2 - 2}{4N} T S_d \frac{p^\epsilon}{\epsilon} + T^2 S_d^2 p^{2\epsilon} \left( \frac{-N^2 + 2}{16N^2} \frac{1}{\epsilon^2} - \frac{N^2}{64} \frac{1}{\epsilon} + \frac{3N^2}{128} \right) + \dots \right]. \quad (109)$$

On the lattice we obtained [neglecting  $O(a^2)$  terms]

$$G_L(T, x, a) = 1 + \frac{N^2 - 1}{2N} T E(x/a) + \frac{N^2 - 1}{2N} \frac{N^2 - 2}{16N} T^2 E(x/a) (1 + 2E(x/a)) + \dots, \quad (110)$$

where

$$E(x/a) = \frac{1}{2\pi} \left( \ln a/x - \gamma_E - \frac{3}{2} \ln 2 \right), \quad (111)$$

$$\begin{aligned} \tilde{G}_L(T, p, a) = & \frac{N^2 - 1}{2N} \frac{T}{p^2} \left[ 1 + \frac{N^2 - 2}{4N} T \left( B(pa) + \frac{1}{4} \right) \right. \\ & \left. + T^2 \left( \frac{-N^2 + 2}{16N^2} B(pa)^2 + \frac{N^4 - 4N^2 + 4}{32N^2} B(pa) - \frac{N^2}{32} C(pa) + \frac{5N^4 - 25N^2 + 30}{768N^2} + \frac{N^2}{32} G_1 \right) + \dots \right], \end{aligned} \quad (112)$$

where

$$\begin{aligned} B(pa) &= \frac{1}{2\pi} \left( \ln pa - \frac{5}{2} \ln 2 \right), \\ C(pa) &= \frac{1}{(2\pi)^2} \left( \ln pa - \frac{5}{2} \ln 2 - \frac{1}{2} \right), \end{aligned} \quad (113)$$

and  $G_1$  is a numerical constant:  $G_1 = 0.04616363$  [26, 27]. The equivalence of the  $SU(2) \times SU(2)$  chiral model to the  $O(4)$   $\sigma$  model allows a check of these expressions; indeed, for  $N = 2$  they must give (and indeed they do) the same results obtained for the corresponding correlation functions in the standard lattice  $O(4)$   $\sigma$  model [26].

On the lattice, neglecting  $O(a^2 \ln^n a)$  terms, the correlation function  $\tilde{G}_L(T, p, a)$  satisfies the renormalization group equation

$$\left[ -a \frac{\partial}{\partial a} + \beta_L(T) \frac{\partial}{\partial T} + \gamma_L(T) \right] \tilde{G}_L(T, p, a) = 0, \quad (114)$$

where the functions  $\beta_L(T)$  and  $\gamma_L(T)$  tell us how the temperature and the field  $U$  should vary with the lattice spacing  $a$  to keep the renormalized quantities fixed:

$$\beta_L(T) \equiv -a \frac{d}{da} T = -b_0 T^2 - b_1 T^3 - b_{2L} T^4 + \dots, \quad (115)$$

$$\gamma_L(T) \equiv a \frac{d}{da} \ln Z_U = \gamma_1 T + \gamma_{2L} T^2 + \gamma_{3L} T^3 + \dots. \quad (116)$$

$Z_U$  is the function entering the renormalization of the two-point function

$$G_R(t, x, \mu) = Z_U(T, a\mu)^{-1} G_L(T, x, a), \quad (117)$$

where  $t$  is the renormalized coupling connected to the temperature by the relation  $T = tZ_t$ , and  $\mu$  is an energy scale. In Eqs. (115) and (116),  $b_0$ ,  $b_1$ , and  $\gamma_1$  are universal coefficients independent of the regularization scheme, and appearing also in the renormalization group equations giving the behavior of the renormalized quantities when varying  $\mu$  keeping the bare quantities fixed:

$$\begin{aligned} b_0 &= \frac{N}{8\pi}, \quad b_1 = \frac{N^2}{128\pi^2}, \\ \gamma_1 &= \frac{N^2 - 1}{4N\pi}. \end{aligned} \quad (118)$$

The coefficients  $b_{2L}$ ,  $\gamma_{2L}$ , and  $\gamma_{3L}$  can be calculated using the procedure described in Ref. [26]. We determine the renormalized functions  $Z_t^{\overline{\text{MS}}}(T, a\mu)$  and  $Z_U^{\overline{\text{MS}}}(T, a\mu)$  that satisfy the equations

$$\begin{aligned} G_R^{\overline{\text{MS}}}(t, x, \mu) &= Z_U^{\overline{\text{MS}}}(T, a\mu)^{-1} G_L(T, x, a), \\ T &= Z_t^{\overline{\text{MS}}}(T, a\mu) t, \end{aligned} \quad (119)$$

where  $t$  and  $G_R^{\overline{\text{MS}}}(t, x, \mu)$  are respectively the coupling and the correlation function renormalized in the  $\overline{\text{MS}}$  scheme. Renormalizing in the  $\overline{\text{MS}}$  scheme the expressions (108) and (109) we find

$$G_R^{\overline{\text{MS}}}(t, x\mu = 2e^{-\gamma_E}) = 1 + O(t^3) ,$$

$$\begin{aligned} \tilde{G}_R^{\overline{\text{MS}}}\left(t, \frac{p}{\mu} = 1\right) \\ = \frac{N^2 - 1}{2N} \frac{t}{p^2} \left[ 1 + \frac{3N^2}{128} \frac{t^2}{(2\pi)^2} + O(t^3) \right] , \end{aligned} \quad (120)$$

where  $\gamma_E$  is the Euler constant. Then by imposing Eq. (119) we obtain

$$Z_t^{\overline{\text{MS}}}(T, a\mu) = 1 + L_1 T + L_2 T^2 + O(T^3) , \quad (121)$$

where

$$\begin{aligned} L_i &= c_i (\ln a\mu + d_i) , \quad c_1 = b_0 , \\ d_1 &= -\frac{5}{2} \ln 2 - \pi \frac{N^2 - 2}{2N^2} , \quad c_2 = b_1 , \\ d_2 &= -\frac{5}{2} \ln 2 + \frac{1}{4} - \pi^2 \left( \frac{2N^4 - 13N^2 + 18}{6N^4} + 4G_1 \right) , \end{aligned} \quad (122)$$

$$\begin{aligned} Z_U^{\overline{\text{MS}}}(T, a\mu) = 1 + M_1 T + \left[ \frac{1}{2} \left( 1 + \frac{b_0}{\gamma_1} \right) M_1^2 \right. \\ \left. - M_1 L_1 \right] T^2 + O(T^3) , \end{aligned} \quad (123)$$

where

$$M_1 = e_1 (\ln a\mu + f_1) , \quad e_1 = \gamma_1 , \quad f_1 = -\frac{5}{2} \ln 2 . \quad (124)$$

The ratio of the  $\Lambda$  parameters  $\Lambda_{\overline{\text{MS}}}$  and  $\Lambda_L$  is given by [15]

$$\frac{\Lambda_{\overline{\text{MS}}}}{\Lambda_L} = \exp(-d_1) = \sqrt{32} \exp\left(\pi \frac{N^2 - 2}{2N^2}\right) . \quad (125)$$

$\gamma_{2_L}$  is easily obtained from Eq. (116):

$$\gamma_{2_L} = b_0 \gamma_1 (f_1 - d_1) = \frac{(N^2 - 1)(N^2 - 2)}{64\pi N^2} . \quad (126)$$

By definition, when keeping the bare quantities  $a$  and  $T$  fixed we must have

$$\begin{aligned} \mu \frac{d}{d\mu} t &= -t \mu \frac{d}{d\mu} \ln Z_t^{\overline{\text{MS}}}(T, a\mu) \\ &= \beta_{\overline{\text{MS}}}(t) = -b_0 t^2 - b_1 t^3 - b_{2_{\overline{\text{MS}}}} t^4 + \dots \end{aligned} \quad (127)$$

and

$$\begin{aligned} \mu \frac{d}{d\mu} \ln Z_U^{\overline{\text{MS}}}(T, a\mu) &= \gamma_{\overline{\text{MS}}}(t) \\ &= \gamma_1 t + \gamma_{2_{\overline{\text{MS}}}} t^2 + \gamma_{3_{\overline{\text{MS}}}} t^3 + \dots , \end{aligned} \quad (128)$$

where  $\beta_{\overline{\text{MS}}}(t)$  and  $\gamma_{\overline{\text{MS}}}(t)$  are, respectively, the  $\beta$  function and the anomalous dimension of the field  $U$  in the  $\overline{\text{MS}}$  renormalization scheme. On the other hand, deriving with respect to  $a$ , keeping the renormalized quantities  $\mu$  and  $t$  fixed, we must obtain the  $\beta$  function and the  $U$  field anomalous dimension defined in Eqs. (115) and (116):

$$\beta_L(T) = -T a \frac{d}{da} \ln Z_t^{\overline{\text{MS}}}(T, a\mu) \quad (129)$$

and

$$\gamma_L(T) = a \frac{d}{da} \ln Z_U^{\overline{\text{MS}}}(T, a\mu) . \quad (130)$$

By comparing the perturbative expansions of Eqs. (127) and (128) with those of Eqs. (129) and (130), the coefficients  $b_{2_L}$  and  $\gamma_{3_L}$  can be written in terms of the quantities introduced in Eq. (121) and the corresponding coefficients  $b_{2_{\overline{\text{MS}}}}$ ,  $\gamma_{2_{\overline{\text{MS}}}}$ , and  $\gamma_{3_{\overline{\text{MS}}}}$ , which have been already calculated [28]:

$$b_{2_{\overline{\text{MS}}}} = \frac{3N^3}{512} \frac{1}{(2\pi)^3} \quad (131)$$

and [29]

$$\begin{aligned} \gamma_{2_{\overline{\text{MS}}}} &= 0 , \\ \gamma_{3_{\overline{\text{MS}}}} &= \frac{3N(N^2 - 1)}{256} \frac{1}{(2\pi)^3} . \end{aligned} \quad (132)$$

Indeed

$$b_{2_L} = b_{2_{\overline{\text{MS}}}} + b_0 b_1 (d_1 - d_0) \quad (133)$$

and

$$\gamma_{3_L} = \gamma_{3_{\overline{\text{MS}}}} + \gamma_1 \left[ b_0^2 (d_1 - f_1)^2 - b_1 (d_2 - f_1) \right] . \quad (134)$$

In particular we find

$$b_{2_L} = \frac{1}{(2\pi)^3} \frac{N^3}{128} \left[ 1 + \pi \frac{N^2 - 2}{2N^2} - \pi^2 \left( \frac{2N^4 - 13N^2 + 18}{6N^4} + 4G_1 \right) \right] . \quad (135)$$

Having calculated  $b_{2_L}$ , we can evaluate the first perturbative correction to the two-loop relationship between the lattice scale  $\Lambda_L$  and the temperature:

$$\begin{aligned} \Lambda_L &= (b_0 T)^{-b_1/b_0^2} \exp\left(-\frac{1}{b_0 T}\right) \left[ 1 + \frac{b_1^2 - b_0 b_{2_L}}{b_0^3} T + O(T^2) \right] \\ &= (8\pi\beta)^{1/2} e^{-8\pi\beta} \left[ 1 + \frac{b_1^2 - b_0 b_{2_L}}{N b_0^3} \beta^{-1} + O(\beta^{-2}) \right] . \end{aligned} \quad (136)$$

In the large  $N$  limit,

$$\frac{b_1^2 - b_0 b_{2L}}{N b_0^3} \xrightarrow{N \rightarrow \infty} 0.060\,509\,5 . \tag{137}$$

In order to solve Eq. (114), let us introduce the dimensionless function  $H_L(T, pa) = p^2 \tilde{G}_L(T, p, a)$ . A formal solution of Eq. (114) is given by

$$H_L(T, pa) = H_L(\Theta, 1) \exp \left( \int_T^\Theta dz \frac{\gamma_L(z)}{\beta_L(z)} \right) , \tag{138}$$

where  $\Theta \equiv \Theta(T, pa)$  satisfies the equation

$$y \frac{\partial}{\partial y} \Theta(T, y) = \beta_L(\Theta) . \tag{139}$$

Defining the function

$$\begin{aligned} z(T) &\equiv \exp \left( \int dT \frac{\gamma_L(T)}{\beta_L(T)} \right) \\ &= T^{-\gamma_1/b_0} \left[ 1 + \frac{\gamma_1 b_1 - \gamma_{2L} b_0}{b_0^2} T + \frac{\gamma_{2L} b_1 b_0^2 + \gamma_1 (b_{2L} b_0 - b_1^2) b_0 - \gamma_{3L} b_0^3 + (\gamma_1 b_1 - \gamma_{2L} b_0)^2}{2 b_0^4} T^2 + O(T^3) \right] , \end{aligned} \tag{140}$$

$H_L(T, pa)$  can be rewritten in the form

$$H_L(T, pa) = z(T)^{-1} z(\Theta) H_L(\Theta, 1) . \tag{141}$$

Solving perturbatively Eq. (139) we find

$$\Theta = \frac{1}{b_0 u} \left[ 1 - \frac{b_1 \ln u}{b_0^2 u} + \frac{b_1^2 \ln u (\ln u - 1) + b_{2L} b_0 - b_1^2}{b_0^4 u^2} + O \left( \frac{\ln^3 u}{u^3} \right) \right] , \tag{142}$$

where  $u = \ln(p/\Lambda_L)$ . The perturbative expansion of  $H_L(\Theta, 1)$  can be obtained from Eq. (112).

In order to get a more accurate description of the approach to asymptotic scaling we performed the change of variables suggested by Parisi [7], defining a new temperature  $T_E$  proportional to the energy:

$$T_E = \frac{8N}{N^2 - 1} E , \quad \beta_E = \frac{1}{N T_E} . \tag{143}$$

The ratio of  $\Lambda_E$ , the  $\Lambda$  parameter of the  $\beta_E$  scheme, and  $\Lambda_L$  is easily obtained from the two-loop term of the energy density:

$$\frac{\Lambda_E}{\Lambda_L} = \exp \left( \pi \frac{N^2 - 2}{4N^2} \right) . \tag{144}$$

Within the  $\beta_E$  scheme, the two-point function  $\tilde{G}^E(T_E, p, a)$  must satisfy the renormalization group equation [neglecting  $O(a^2 \ln^n a)$  terms]

$$\left[ -a \frac{\partial}{\partial a} + \beta_E(T_E) \frac{\partial}{\partial T_E} + \gamma_E(T_E) \right] \tilde{G}_E(T_E, p, a) = 0 . \tag{145}$$

The  $\beta$  function of the  $\beta_E$  scheme can be written in the form

$$\beta_E(T_E) \equiv -a \frac{d}{da} T_E = \frac{8N^2}{N^2 - 1} C(T) \beta_L(T) , \tag{146}$$

where

$$C(T) = \frac{1}{N} \frac{dE}{dT} \tag{147}$$

is the specific heat and  $T$  must be considered as a function of  $T_E$ . Expanding perturbatively Eq. (146) and using Eq. (104) one finds

$$b_{2E} = b_{2L} + N^2 b_0 (a_2 - a_1^2) + N b_1 a_1 . \tag{148}$$

The scale  $\Lambda_E$  is related to the variable  $\beta_E$  by

$$\begin{aligned} \Lambda_E &= (8\pi\beta_E)^{1/2} \\ &\times e^{-8\pi\beta_E} \left[ 1 + \frac{b_1^2 - b_0 b_{2E}}{N b_0^3} \beta_E^{-1} + O(\beta_E^{-2}) \right] \end{aligned} \tag{149}$$

In the large  $N$  limit

$$\frac{b_1^2 - b_0 b_{2E}}{N b_0^3} \xrightarrow{N \rightarrow \infty} -0.040\,09 . \tag{150}$$

The function  $\gamma_E(T_E)$  is easily obtained from the relation

$$\gamma_E(T_E) = \gamma_L(T) , \tag{151}$$

and therefore

$$\begin{aligned} \gamma_{2E} &= \gamma_{2L} - \gamma_1 N a_1 = \frac{(N^2 - 1)(N^2 - 2)}{128\pi N^2} , \\ \gamma_{3E} &= \gamma_{3L} - 2\gamma_{2L} N a_1 + \gamma_1 N^2 (2a_1^2 - a_2) . \end{aligned} \tag{152}$$

The renormalization equation (145) can be solved fol-

lowing the same procedure used in the standard scheme. Defining  $H_E(T_E, pa) = p^2 \tilde{G}_E(T_E, p, a)$  we obtain

$$H_E(T_E, pa) = z_E(T_E)^{-1} z_E(\Theta_E) H(\Theta_E, 1) , \quad (153)$$

where

$$z_E(T) \equiv \exp \left( \int dT_E \frac{\gamma_E(T_E)}{\beta_E(T_E)} \right) , \quad (154)$$

and  $\Theta_E \equiv \Theta_E(T_E, pa)$  satisfies the equation

$$y \frac{\partial}{\partial y} \Theta_E(T_E, y) = \beta_E(\Theta_E) , \quad (155)$$

whose perturbative solution is obtained from Eq. (142) by substituting  $b_{2L} \rightarrow b_{2E}$  and  $\Lambda_L \rightarrow \Lambda_E$ . The perturbative expansion of  $H_E(\Theta_E, 1)$  can be found by reexpressing perturbatively  $T$  in terms of  $T_E$  in the right-hand side (RHS) of Eq. (112).

Notice that having performed only a coupling redefinition  $T \rightarrow T_E$ , it must be  $\tilde{G}_E(T_E, p, a) = \tilde{G}_L(T, p, a)$ . But when evaluating them at some finite order in perturbation theory we get different results, which are different approximations of the same quantity.

## V. NUMERICAL RESULTS

In order to investigate numerically the large  $N$  limit of  $SU(N) \times SU(N)$  chiral models, we performed Monte Carlo simulations for several large values of  $N$ . We will show numerical results for  $N = 6, 9, 15, 21, 30$ . In Ref. [4]

some results at  $N = 6, 9, 15$  were already presented, and in the following we will use some of those data. A summary of our new large statistics Monte Carlo results is presented in Table I.

In our simulations we used local algorithms containing overrelaxation procedures. We implemented the Cabibbo-Marinari algorithm [30] to upgrade  $SU(N)$  matrices by updating their  $SU(2)$  subgroups. In most cases, the  $SU(2)$  updates were performed by using the overheat-bath algorithm [31] (for the ‘‘heat bath’’ part of it we used the Kennedy-Pendleton algorithm [32]). A sweep consisted in updating a number of  $SU(2)$  subgroups at all sites of the lattice. For relatively small values of  $N$  ( $N \lesssim 6$ , say) we chose to update the  $N - 1$  diagonal subsequent  $SU(2)$  subgroups of each  $SU(N)$  matrix variable. At larger  $N$  we found more efficient to select randomly the  $SU(2)$  subgroups among the  $\frac{N(N-1)}{2}$  subgroups acting on each  $2 \times 2$  submatrix. At each site the  $SU(2)$  subgroup identified by the indices  $i, j$  ( $1 \leq i < j \leq N$ ) was updated with a probability  $P = \frac{2\alpha}{N-1}$ , so that the average number of  $SU(2)$  updates per  $SU(N)$  site variable was  $\bar{n} = \alpha N$ . In our simulations we always chose  $\alpha \lesssim 1$ , decreasing  $\alpha$  when increasing  $N$ . At  $N = 21, 30$  we used  $\alpha = 0.5$ . (We should say that our choices of the values of  $\alpha$  came from a rough study of the performances of the algorithm since the construction of the ‘‘most’’ efficient algorithm was not among our principal purposes.) Such an algorithm turns out to be quite efficient in the range of  $N$  and  $\beta$  (and correlation lengths) we considered.

TABLE I. Summary of the numerical results. Errors of data marked by an asterisk could be underestimated. When more than one lattice size appears, the corresponding results were obtained collecting data of simulations at the reported lattice sizes (which were, in all cases, in agreement within the errors).

| $\beta$ | $N$ | $L$         | $E$          | $C$       | $\chi$     | $\xi_G$   | $\xi_w$    | $\xi_G/\xi_w$ | $\xi_d/\xi_w$ |
|---------|-----|-------------|--------------|-----------|------------|-----------|------------|---------------|---------------|
| 0.20    | 15  | 18,21       | 0.781405(7)  | 0.0527(3) | 2.9380(7)  | 0.786(3)  | 0.8360(4)  | 0.941(3)      | 0.9724(4)     |
| 0.20    | 21  | 18,21       | 0.781427(7)  | 0.0527(3) | 2.9381(5)  | 0.788(2)  | 0.8358(3)  | 0.943(2)      | 0.9726(4)     |
| 0.20    | 30  | 18          | 0.781422(10) | 0.0522(6) | 2.9379(8)  | 0.787(2)  | 0.834(2)   | 0.944(3)      | 0.973(2)      |
| 0.28    | 15  | 18,24       | 0.65000(5)   | 0.191(5)  | 7.249(6)   | 1.560(4)  | 1.587(2)   | 0.9834(13)    | 0.9922(6)     |
| 0.28    | 21  | 18,24       | 0.65290(3)   | 0.170(3)  | 7.069(5)   | 1.532(3)  | 1.5605(10) | 0.9819(11)    | 0.9917(4)     |
| 0.28    | 30  | 18          | 0.65352(3)   | 0.163(4)  | 7.032(5)   | 1.529(3)  | 1.5544(15) | 0.9837(12)    | 0.9916(5)     |
| 0.29    | 9   | 24,30       | 0.58772(7)   | 0.412(5)  | 13.32(3)   | 2.369(10) | 2.395(9)   | 0.9889(9)     | 1.000(2)      |
| 0.29    | 30  | 21          | 0.63058(3)   | 0.208(6)  | 8.497(8)   | 1.740(4)  | 1.765(5)   | 0.9857(7)     | 0.992(2)      |
| 0.295   | 9   | 24,30,36,42 | 0.56278(6)   | 0.444(5)  | 18.03(4)   | 2.913(9)  | 2.949(13)  | 0.988(2)      | 0.996(3)      |
| 0.30    | 15  | 24,30,36,42 | 0.56806(4)   | 0.68(2)   | 16.574(13) | 2.742(5)  | 2.767(9)   | 0.9907(10)    | 1.000(1)      |
| 0.30    | 21  | 24          | 0.58799(14)  | 0.65(3)   | 12.91(3)   | 2.309(7)  | 2.333(7)   | 0.9899(7)     | 0.997(2)      |
| 0.30    | 30  | 24          | 0.59927(8)   | 0.38(2)   | 11.35(2)   | 2.114(7)  | 2.137(10)  | 0.989(2)      | 0.993(3)      |
| 0.3025  | 21  | 30          | 0.56525(19)  | 1.02(5)*  | 17.02(5)   | 2.786(10) | 2.813(12)  | 0.9903(8)     | 0.997(2)      |
| 0.3025  | 30  | 30          | 0.58479(10)  | 0.79(5)*  | 13.24(3)   | 2.338(7)  | 2.362(9)   | 0.990(2)      | 0.999(2)      |
| 0.304   | 30  | 24          | 0.5627(4)    | 2.6(3)*   | 17.52(9)   | 2.839(8)  | 2.866(11)  | 0.9907(13)    | 0.998(2)      |
| 0.305   | 15  | 36          | 0.53415(8)   | 0.52(2)   | 26.86(7)   | 3.782(16) | 3.82(3)    | 0.989(3)      | 0.996(4)      |
| 0.305   | 21  | 30          | 0.54098(10)  | 0.73(3)   | 24.14(6)   | 3.523(10) | 3.57(2)    | 0.988(2)      | 0.998(3)      |
| 0.305   | 30  | 30          | 0.54658(14)  | 1.05(10)* | 22.13(5)   | 3.320(12) | 3.35(2)    | 0.990(2)      | 1.000(3)      |
| 0.31    | 6   | 60          | 0.48187(2)   | 0.257(3)  | 65.2(2)    | 6.63(3)   | 6.69(4)    | 0.9909(10)    | 1.003(3)      |
| 0.31    | 9   | 48          | 0.50030(4)   | 0.302(6)  | 47.25(12)  | 5.44(3)   | 5.49(5)    | 0.9908(17)    | 0.998(5)      |
| 0.31    | 15  | 45          | 0.51178(4)   | 0.354(7)  | 39.06(10)  | 4.80(2)   | 4.84(3)    | 0.9911(12)    | 1.001(2)      |
| 0.31    | 21  | 42          | 0.51548(6)   | 0.41(2)   | 36.66(12)  | 4.61(2)   | 4.65(3)    | 0.9915(10)    | 0.999(3)      |
| 0.32    | 9   | 66          | 0.47234(3)   | 0.252(3)  | 82.4(3)    | 7.70(4)   | 7.78(7)    | 0.990(2)      | 1.002(3)      |
| 0.32    | 15  | 66          | 0.48072(2)   | 0.264(5)  | 70.5(3)    | 6.96(4)   | 7.04(4)    | 0.9892(11)    | 1.000(3)      |
| 0.33    | 6   | 102         | 0.43706(2)   | 0.212(3)  | 175.3(2.0) | 12.13(16) | 12.23(21)  | 0.991(3)      | 1.001(9)      |

An important class of observables of the  $SU(N) \times SU(N)$  chiral models can be constructed from the correlation function  $G(x-y) = \langle \frac{1}{N} \text{Re Tr} [U(x)U(y)^\dagger] \rangle$ .

The inverse mass gap  $\xi_w$  is extracted from the long distance behavior of the zero space momentum (wall-wall) correlation function constructed with  $G(x)$ . Moreover we measured the diagonal wall-wall correlation length  $\xi_d$  to test rotation invariance.  $M \equiv 1/\xi_w$  should reproduce in the continuum limit the mass of the fundamental state. Another definition of correlation length  $\xi_G$  comes from the second moment of  $G(x)$ . In the small momentum regime,  $p^2 \xi_G^2 \ll 1$ , we expect the behavior

$$\tilde{G}(p) \simeq \frac{Z_G}{M_G^2 + p^2}, \quad (156)$$

where  $\tilde{G}(p)$  is the Fourier transform of  $G(x)$ ,  $M_G \equiv \xi_G^{-1}$  and  $Z_G$  is a constant. On the lattice we can use the two lowest components of  $\tilde{G}(p)$  to obtain the following definition of  $\xi_G$ :

$$\xi_G^2 = \frac{1}{4 \sin^2 \pi/L} \left[ \frac{\tilde{G}(0,0)}{\tilde{G}(0,1)} - 1 \right], \quad (157)$$

where  $\tilde{G}(k_x, k_y)$  is the lattice Fourier transform of  $G(x)$ .

In Table I we present data for the energy density  $E$ , the specific heat  $C \equiv \frac{1}{N} \frac{dE}{dT}$ , the magnetic susceptibility  $\chi \equiv \tilde{G}(0)$ , the correlation lengths  $\xi_G$  and  $\xi_w$ , and the dimensionless ratios  $\xi_G/\xi_w$  and  $\xi_d/\xi_w$ . Data analyses were performed by using the jackknife method. For comparison, in Table II we report some strong coupling results at  $N = \infty$  obtained in Secs. II and III.

Finite size effects were carefully checked (see also Ref. [4]). Finite size systematic errors in evaluating infinite volume quantities should be smaller than the statistical errors of all numerical results presented in this paper. In all cases we used lattice sizes  $L \gtrsim 8.5\xi_G$ .

Figures 1, 2, and 3 show the Monte Carlo data of the energy density and the specific heat respectively at  $N = 6$ ,  $N = 9$ , and  $N = 15$ , with the corresponding strong and weak coupling series calculated in the previous sections. As in other asymptotically free models, at all values of  $N$  the specific heat shows a peak, connecting the two different asymptotic behaviors: monotonically increasing in the strong coupling region and decreasing at large  $\beta$ . The position of the peak of  $C$  should give an estimate of the strong coupling convergence radius.

As already observed in Ref. [4] and confirmed by our more recent data at  $N > 15$ , increasing  $N$  the peak of  $C$  moves slightly toward higher  $\beta$  values and becomes more and more pronounced, not showing any apparent conver-

TABLE II. Strong coupling results at  $N = \infty$ .

| $\beta$ | $E$       | $C$      | $\chi$  | $\xi_G$ | $\xi_w$ |
|---------|-----------|----------|---------|---------|---------|
| 0.20    | 0.7814220 | 0.052534 | 2.93042 | 0.78782 | 0.83545 |
| 0.25    | 0.7090132 | 0.101253 | 4.53372 | 1.14095 | 1.17077 |
| 0.28    | 0.6556834 | 0.154155 | 6.24295 | 1.52097 | 1.51721 |
| 0.29    | 0.6352185 | 0.179292 | 7.01908 | 1.71684 | 1.68254 |
| 0.30    | 0.6129234 | 0.210053 | 7.93319 | 1.98464 | 1.88946 |

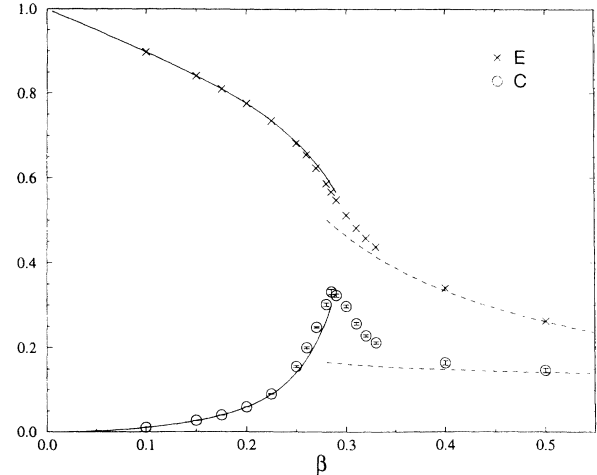


FIG. 1. Energy and specific heat vs  $\beta$  for  $N = 6$ . The solid and dashed lines represent, respectively, the strong coupling [up to  $O(\beta^{12})$  for  $E$  and up to  $O(\beta^{13})$  for  $C$ ] and the weak coupling series.

gence to a finite value. This might be an indication of a phase transition at  $N = \infty$ , which a rough extrapolation would place at  $\beta_{\text{sing}} \simeq 0.305$ , with an uncertainty of few per mille. From  $N = 6$  up to  $N = 30$ , we found the position of the peak to be very stable with respect to the correlation length: It occurs at  $\xi_G \simeq 2.80$  for  $N \geq 6$ .

Rotation invariance at distances  $d \gtrsim \xi$  is checked by measuring the ratio  $\xi_d/\xi_w$ . In Fig. 4 the ratio  $\xi_d/\xi_w$  is plotted versus  $\xi_G$ . Data show effective rotation invariance already for  $\xi_G \simeq 2$ . At smaller correlation lengths, discrepancies from 1 are well reproduced by the Gaussian model (see Appendix B), which predicts

$$\frac{\xi_d}{\xi_w} = \frac{\ln \left( \frac{1}{2\xi_G} + \sqrt{1 + \frac{1}{4\xi_G^2}} \right)}{\sqrt{2} \ln \left( \frac{1}{2\sqrt{2}\xi_G} + \sqrt{1 + \frac{1}{8\xi_G^2}} \right)}. \quad (158)$$

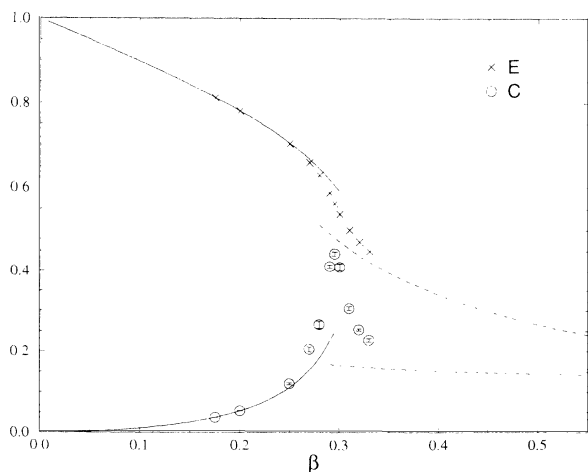


FIG. 2. Energy and specific heat vs  $\beta$  for  $N = 9$ . The solid and dashed lines represent, respectively, the strong coupling [up to  $O(\beta^{14})$  for  $E$  and up to  $O(\beta^{15})$  for  $C$ ] and the weak coupling series.

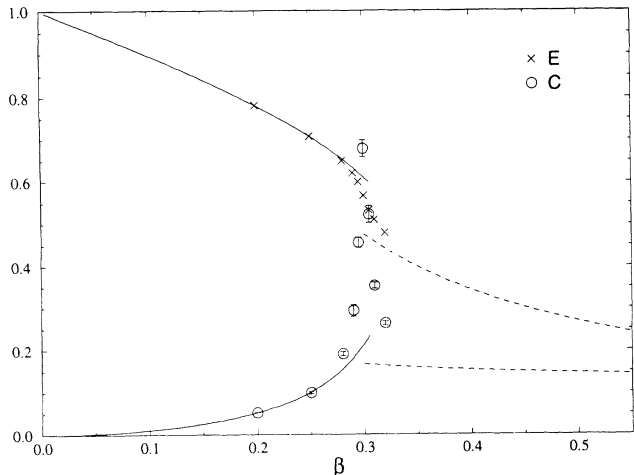


FIG. 3. Energy and specific heat vs  $\beta$  for  $N = 15$ . The solid and dashed lines represent, respectively, the strong coupling [up to  $O(\beta^{14})$  for  $E$  and up to  $O(\beta^{15})$  for  $C$ ] and the weak coupling series.

Other important tests of scaling are based on the stability of dimensionless physical quantities, such as the ratio  $\xi_G/\xi_w$ , which is in general different from one. Data of  $\xi_G/\xi_w$  are shown in Fig. 5. Within statistical errors of few per mille,  $\xi_G/\xi_w$  is stable for  $\xi_G \gtrsim 2$ , and independent of  $N$  for  $N \geq 6$ , showing a rapid convergence to the  $N = \infty$  value. We conclude that, in the large  $N$  limit,

$$\frac{\xi_G}{\xi_w} \simeq 0.991, \tag{159}$$

with an uncertainty of about one per mille. As shown in Fig. 5, the comparison with the Gaussian model prediction

$$\frac{\xi_G}{\xi_w} = 2\xi_G \ln \left( \frac{1}{2\xi_G} + \sqrt{1 + \frac{1}{4\xi_G^2}} \right) \tag{160}$$

is very good at small correlation lengths  $\xi_G \lesssim 2$ , but

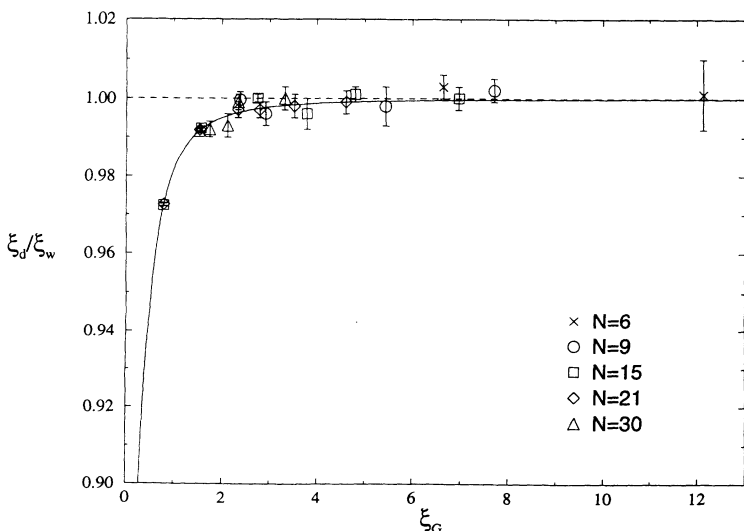


FIG. 4. The ratio  $\xi_d/\xi_w$  vs  $\xi_G$ . The solid line represents the Gaussian prediction (158).

then discrepancies arise since in the Gaussian case the continuum limit is 1.

Notice that scaling is observed even around the peak of the specific heat, even though its behavior with respect to  $N$  suggests the existence of a phase transition at  $N = \infty$ . In a sense, at  $N = \infty$  the modes responsible for the phase transition should be effectively decoupled from those determining the physical continuum limit, meant as the renormalization group trajectories where dimensionless quantities are stable.

Similar considerations hold for the approach to asymptotic scaling, when using a “good” definition of temperature. A “good” definition of temperature turns out to be  $T_E \propto E$  [see Eq. (143)], whose corresponding specific heat is, by definition, constant. From the Monte Carlo data of  $M \equiv 1/\xi_w$  and assuming the exact result (3), we extract the effective  $\Lambda$  parameters  $\Lambda_L(N, \beta)$  and  $\Lambda_E(N, \beta_E)$ :

$$\Lambda_{L,E} = \left( \frac{\Lambda_{L,E}}{M} \right) M = \frac{M}{R_{L,E}}, \tag{161}$$

where  $R$  is the mass- $\Lambda$  parameter ratio obtained by using Eq. (3):  $R_{L,E} = R_{\overline{MS}}(\Lambda_{\overline{MS}}/\Lambda_{L,E})$ . Figure 6 shows the ratio  $\Lambda_L(N, \beta)/\Lambda_{L,2l}(N, \beta)$ , where  $\Lambda_{L,2l}(N, \beta)$  is the corresponding two-loop function:  $\Lambda_{L,2l}(N, \beta) = (8\pi\beta)^{1/2} e^{-8\pi\beta}$ . Around the region where the specific heat has a peak, also  $\Lambda_L(N, \beta)/\Lambda_{L,2l}(N, \beta)$  shows a peak, whose shape tends to be singular when  $N \rightarrow \infty$  for  $\beta_{\text{sing}} \simeq 0.305$ , consistently with the extrapolation from the specific heat. The observed peaks in the ratio  $\Lambda_L(N, \beta)/\Lambda_{L,2l}(N, \beta)$  correspond to dips in the  $\beta$  functions, and the singularity of  $\Lambda_L(\infty, \beta)$  would reveal a singularity of the  $N = \infty$   $\beta$  function. The similarity with the behavior of the specific heat suggests that the peak of  $C$  and the dip of the  $\beta$  function have the same origin. They are presumably related to complex  $\beta$  singularities of the partition function close to the real axis [9] that for  $N \rightarrow \infty$  should finally pinch the real axis.

As already observed in other contexts (see for example [33–35]), the approach to asymptotic scaling gets an

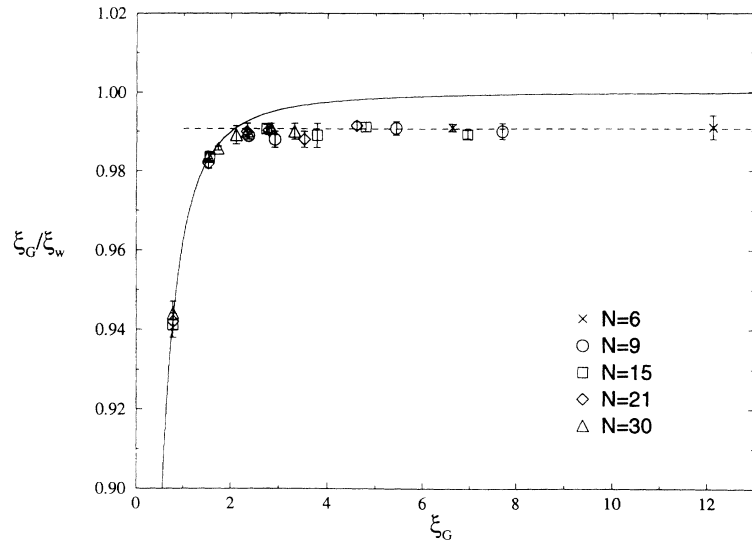


FIG. 5. The ratio  $\xi_G/\xi_w$  vs  $\xi_G$ . The solid line represents the Gaussian prediction (160). The dashed line is the result of a fit.

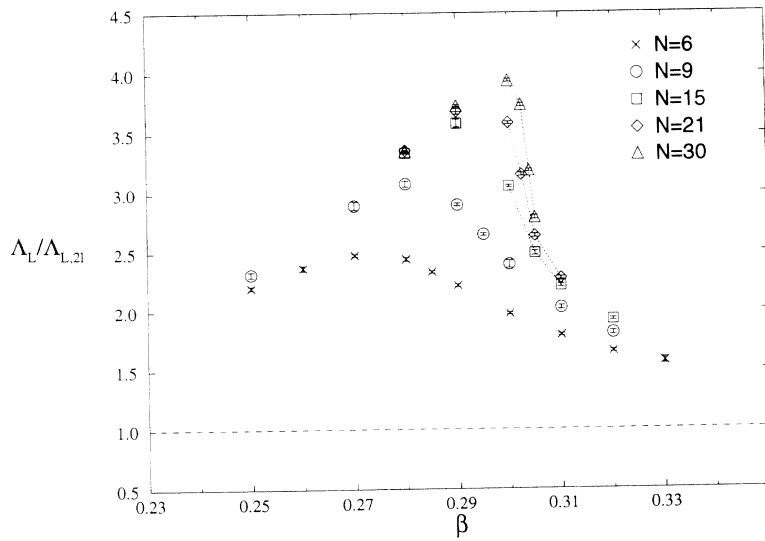


FIG. 6.  $\Lambda_L(N, \beta)/\Lambda_{L,2l}(N, \beta)$  vs  $\beta$ . The dotted lines connecting different sets of data are drawn to guide the eyes.

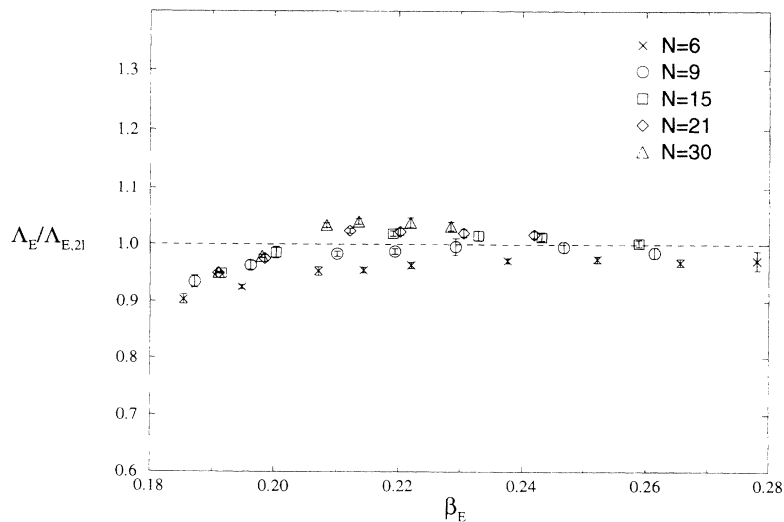


FIG. 7.  $\Lambda_E(N, \beta_E)/\Lambda_{E,2l}(N, \beta_E)$  vs  $\beta_E$ .

impressive improvement in the  $\beta_E$  scheme, where the dip of the  $\beta$  function disappears at all values of  $N$ . Figure 7 shows the ratio  $\Lambda_E(N, \beta_E)/\Lambda_{E,2l}(N, \beta_E)$ , where  $\Lambda_E(N, \beta_E)$  is the effective  $\Lambda$  parameter of the  $\beta_E$  scheme, and  $\Lambda_{E,2l}(N, \beta_E)$  is the corresponding two-loop function. Unlike  $\Lambda_L(N, \beta)$ ,  $\Lambda_E(N, \beta_E)$  appears to approach a smooth function  $\Lambda_E(\infty, \beta_E)$  that is well approximated by the two-loop formula  $\Lambda_E(\infty, \beta_E) \simeq (8\pi\beta_E)^{1/2} e^{-8\pi\beta_E}$  even around the peak of the specific heat, which is placed at  $\beta_E \simeq 0.220$  for  $N \geq 6$  (the peak position being much more stable in  $N$  when described by the variable  $\beta_E$  instead of  $\beta$ ).

In Sec. IV we found that in the standard and the energy schemes the linear corrections to the two-loop lattice scale in Eqs. (136) and (149) are small and of the same order of magnitude, although of opposite sign. Therefore perturbative arguments do not explain the failure of the standard and the success of the  $\beta_E$  scheme with respect to achieving asymptotic scaling. We believe the flattening of the specific heat to be the key feature of the  $\beta_E$  scheme. A coupling transformation eliminating the peak of the specific heat should move the complex  $\beta$  singularities away from the real axis, and therefore improve the approach to asymptotic scaling.

The above considerations are consistent with the relationship (146). Indeed, assuming that at  $N = \infty$  the  $\beta$  function of the  $\beta_E$  scheme is not singular (as data seem to show) and the specific heat has a divergence at  $\beta_{\text{sing}}$ , then Eq. (146) predicts a singularity in the  $N = \infty$   $\beta$  function of the standard scheme at  $\beta_{\text{sing}}$ .

Asymptotic scaling within the  $\beta_E$  scheme can be also checked by using the strong coupling estimates of  $E$ ,  $\xi_w$ ,

$$\begin{aligned} Z_G &= c(N) N^{\gamma_1/b_0} z(T)^{-1} = c(N) \beta^{-\gamma_1/b_0} \left[ 1 + O\left(\frac{1}{\beta}\right) \right] \\ &= c(N) N^{\gamma_1/b_0} z_E(T_E)^{-1} = c(N) \beta_E^{-\gamma_1/b_0} \left[ 1 + O\left(\frac{1}{\beta_E}\right) \right], \end{aligned} \quad (162)$$

where the function  $z(T)$  and  $z_E(T_E)$  were defined in Eqs. (140) and (154), and  $c(N)$  is a constant independent of the regularization scheme. In Figs. 9 and 10 we plotted, respectively, the quantities  $c_L(N, \beta) \equiv Z_G \beta^{\gamma_1/b_0}$  and  $c_E(N, \beta_E) \equiv Z_G \beta_E^{\gamma_1/b_0}$ . Figure 9 shows also the strong coupling estimate of  $c_L(\infty, \beta)$  obtained from Eq. (84).  $c_L(N, \beta)$  appears to be far from being approximately constant. It tends to be singular when  $N \rightarrow \infty$  at  $\beta_{\text{sing}} \simeq 0.305$ , consistently with the previous estimates of the singularity. On the contrary,  $c_E(N, \beta_E)$  shows a much smoother behavior and a rapid convergence at large  $N$ . Again, perturbative arguments do not help to explain such different behaviors, since perturbative corrections are small for both schemes. Indeed from Eqs. (140) and (154) we can derive the following relationships at  $N = \infty$ :

$$\begin{aligned} c_L(\infty, \beta) &= c(\infty) \left[ 1 + \frac{0.08521}{\beta} + \frac{0.01314}{\beta^2} \right. \\ &\quad \left. + O\left(\frac{1}{\beta^3}\right) \right] \end{aligned} \quad (163)$$

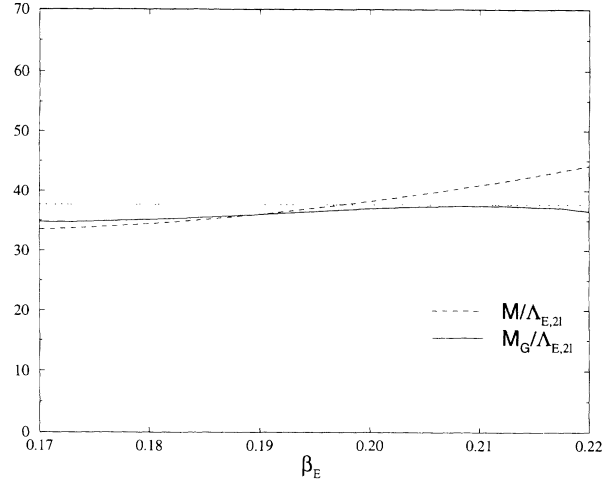


FIG. 8. Asymptotic scaling test by using strong coupling estimates. The dotted line represents the exact result (3).

and  $\xi_G$ . In Fig. 8 we show the results using the strong coupling series obtained in Secs. II and III [ $E$  up to  $O(\beta^{14})$ ,  $\xi_w$  up to  $O(\beta^8)$ , and  $\xi_G$  up to  $O(\beta^9)$ ] at  $N = \infty$ , and for  $\beta_E < 0.220$ , which should be the approximate position of the specific heat singularity. The comparison with the predicted mass- $\Lambda$  parameter ratio is very good, especially for  $\xi_G$  whose series has alternate signs.

Another quantity we found to be very sensitive to the change of variable  $T \rightarrow T_E$  is the renormalization constant  $Z_G$  introduced in Eq. (156). Its dependence on  $\beta$  can be determined by renormalization group considerations; indeed, it must satisfy Eq. (116). One finds

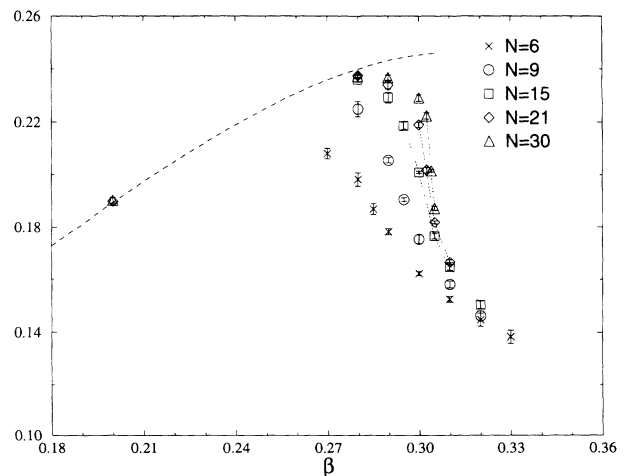


FIG. 9.  $c_L = Z_G \beta^{\gamma_1/b_0}$  vs  $\beta$ . The dashed line shows the strong coupling series for  $N = \infty$ . The dotted lines connecting different sets of data are drawn to guide the eyes.

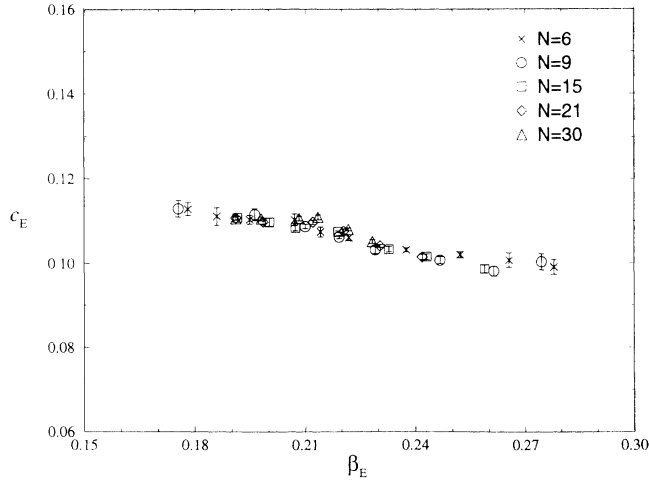


FIG. 10.  $c_E = Z_G \beta_E^{\gamma_1/b_0}$  vs  $\beta_E$ .

and

$$c_E(\infty, \beta_E) = c(\infty) \left[ 1 + \frac{0.02271}{\beta_E} + \frac{0.00079}{\beta_E^2} + O\left(\frac{1}{\beta_E^3}\right) \right]. \quad (164)$$

We could get an estimate of  $c(\infty)$  from the data at the largest available  $\beta_E$  values, obtaining  $c(\infty) \simeq 0.10$  [the perturbative corrections in Eq. (164) are about 10% at  $\beta_E \simeq 0.25$ ].

In Sec. III we found that at large  $N$  the correlation function breaks the Gaussian form at relatively high orders in the strong coupling expansion. Therefore in the very strong coupling domain,  $\tilde{G}(k)$  should be well approximated by Eq. (156) everywhere and not only for  $k^2 \ll M_G^2$ . When the Gaussian approximation works we should find

$$M(k) \equiv \frac{\tilde{G}(k)}{\tilde{G}(0)} (M_G^2 + \hat{k}^2) \simeq 1. \quad (165)$$

Figure 11 shows the components  $(k, 0)$  and  $(k, k)$  of

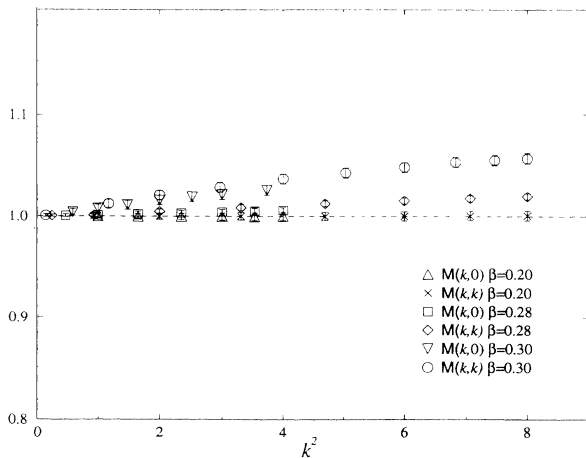


FIG. 11.  $M(k, 0)$  and  $M(k, k)$  vs  $\hat{k}^2$  at  $N = 30$ .

$M(k_1, k_2)$  at  $N = 30$  and for various values of  $\beta$  chosen inside the expected convergence region of the strong coupling expansion. As expected from the strong coupling considerations, at  $\beta = 0.20$  the propagator is effectively Gaussian. Discrepancies, although small, are clear for  $\beta \geq 0.28$ , especially in the diagonal components.

In order to study the continuum limit of  $\tilde{G}(k)$ , we consider the dimensionless function

$$L(k; \beta, N) \equiv \frac{\tilde{G}(0; \beta, N)}{\tilde{G}(k; \beta, N)} - 1. \quad (166)$$

$L(k; \beta, N)$  is renormalization group invariant and, therefore, for  $k^2 a^2 \lesssim 1$

$$L(k; \beta, N) \simeq \bar{L}(k^2 \xi_G^2, N), \quad (167)$$

the function  $\bar{L}(y, N)$  being independent of  $\beta$ . Notice that in the Gaussian model we would have  $\bar{L}(y) = y$ . In Figs. 12 and 13 we plotted the components  $(k, 0)$  and  $(k, k)$  of  $L(k_1, k_2; \beta, N)$  versus  $k^2 \xi_G^2$  obtained respectively at  $N = 6$  for  $\beta = 0.31$  and  $\beta = 0.33$ , and at  $N = 9$  for  $\beta = 0.31$  and  $\beta = 0.32$ . All sets of data follow a single curve for  $k^2 \xi_G^2 \lesssim \xi_G^2/a^2$ , which must be the continuum function  $\bar{L}(y, N)$  at the given  $N$ . Then discrepancies, i.e., scaling violations, arise. Comparing data at different  $\beta$ , we also learn that (i) when there is rotation invariance at a scale  $p$ , i.e.,  $L(p, 0; \beta, N) \simeq L(p/\sqrt{2}, p/\sqrt{2}; \beta, N)$ , then  $L(p; \beta, N) \simeq \bar{L}(p^2 \xi_G^2, N)$ ; (ii) the diagonal components  $L(k, k; \beta, N)$  are closer to the continuum limit than the  $L(k, 0; \beta, N)$  ones.

Figure 14 gathers data of  $L(k, k; \beta, N)$  at different values of  $N$  and  $\beta$ . At relatively low values of  $k^2 \xi_G^2$ , all sets of data follow approximately a single curve, showing that  $\bar{L}(y, N)$  rapidly converges to its large  $N$  limit.  $N = 6, 9$  data give already a good approximation of  $\bar{L}(y; \infty)$ . At larger  $k^2 \xi_G^2$ , the scattering of the curves for different  $N$  is essentially due to scaling violations, because we used data at different  $\xi_G$ .

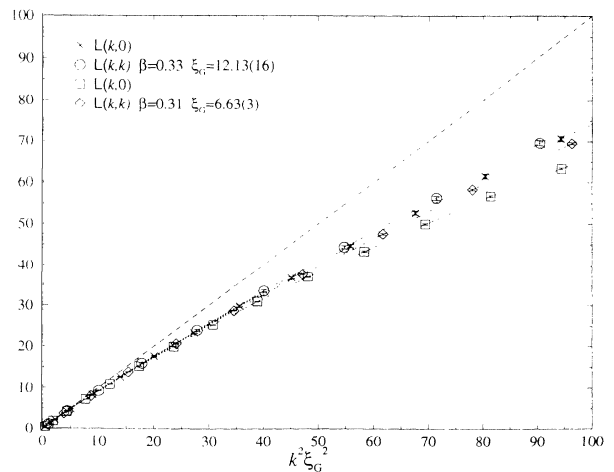


FIG. 12.  $L(k, 0)$  and  $L(k, k)$  vs  $k^2 \xi_G^2$  at  $N = 6$  and for  $\beta = 0.31$  and  $\beta = 0.33$ . The dotted lines connecting different sets of data are drawn to guide the eyes. The dashed line represents the Gaussian prediction.

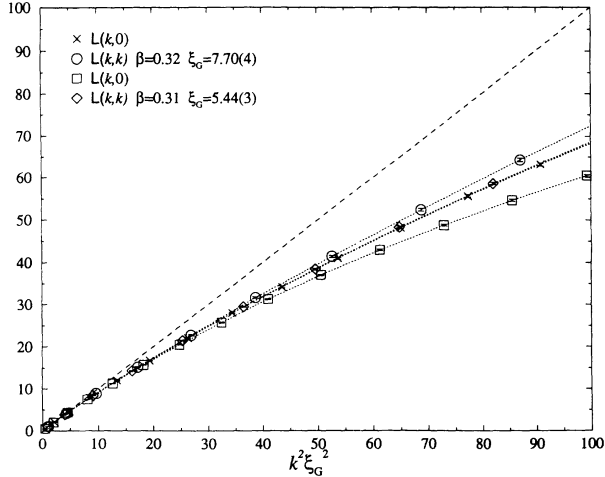


FIG. 13.  $L(k,0)$  and  $L(k,k)$  vs  $k^2 \xi_G^2$  at  $N = 9$  and for  $\beta = 0.31$  and  $\beta = 0.32$ . The dotted lines connecting different sets of data are drawn to guide the eyes. The dashed line represents the Gaussian prediction.

The extrapolation of  $\bar{L}(y, N)$  to negative  $y$  should provide another estimate of the ratio  $M/M_G \equiv \xi_G/\xi_w$ . The solution  $y_0$  of the mass gap equation  $\bar{L}(y) + 1 = 0$  is  $y_0 = -M^2/M_G^2$ . At sufficiently small  $y$ ,  $\bar{L}(y, \infty)$  shows an approximate Gaussian behavior; indeed, for  $y \lesssim 5$  it is well reproduced by a polynomial function  $y + by^2$  with  $b$  very small:  $b \simeq 0.01$ . By using this polynomial function to extrapolate, we find  $y_0 \simeq -1$  within 1%, consistently with the more precise estimate (159).

We finally compare the Monte Carlo data of  $\tilde{G}(k)$  with the perturbative solutions  $\tilde{G}(k)_p$  of the renormalization group equations (138) and (153). In Figs. 15 and 16 we show data, respectively, at  $N = 6$  ( $\beta = 0.33$ ) and  $N = 9$  ( $\beta = 0.32$ ), with their corresponding renormalization group equation solutions at the lowest order and at the next two orders, calculated in the standard and the  $\beta_E$  schemes (see Sec. IV). In particular the lowest order solution of the renormalization group equation for  $\tilde{G}(k)$  is

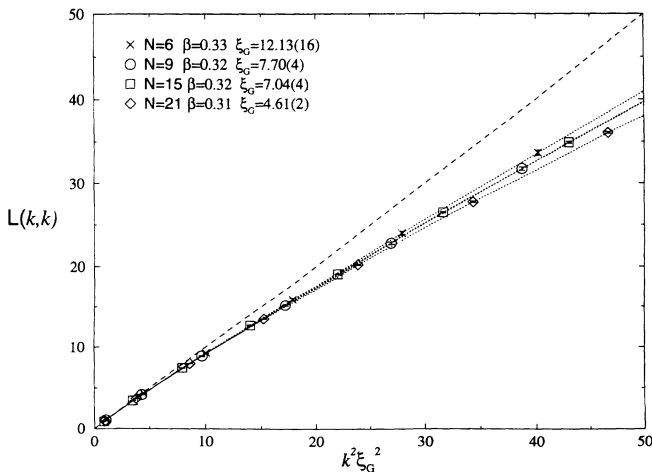


FIG. 14.  $L(k,k)$  vs  $k^2 \xi_G^2$ .

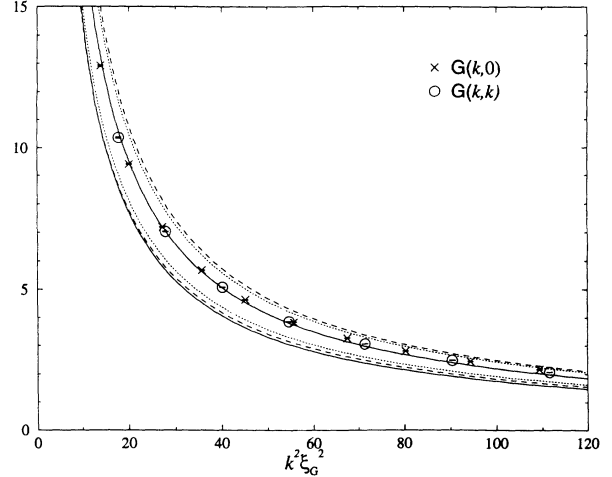


FIG. 15.  $G(k,0)$  and  $G(k,k)$  vs  $k^2 \xi_G^2$  at  $N = 6$  and  $\beta = 0.33$ . The low and high sets of lines (solid, dashed, and dotted) show, respectively, the renormalization group predictions of the standard and the  $\beta_E$  schemes. Solid, dashed, and dotted lines represent, respectively, the lowest, and the one and two next order perturbative solutions.

$$\tilde{G}(k)_{p,1} = \left( \frac{N^2 - 1}{2N} \right) \frac{T^{\gamma_1/b_0}}{k^2} \left( \frac{b_0}{2} \ln \frac{k^2}{\Lambda_L^2} \right)^{\gamma_1/b_0 - 1} \quad (168)$$

in the standard scheme and

$$\tilde{G}(k)_{p,1} = \left( \frac{N^2 - 1}{2N} \right) \frac{T_E^{\gamma_1/b_0}}{k^2} \left( \frac{b_0}{2} \ln \frac{k^2}{\Lambda_E^2} \right)^{\gamma_1/b_0 - 1} \quad (169)$$

in the  $\beta_E$  scheme. In  $\tilde{G}(k)_p$  the scale is provided by the relationship

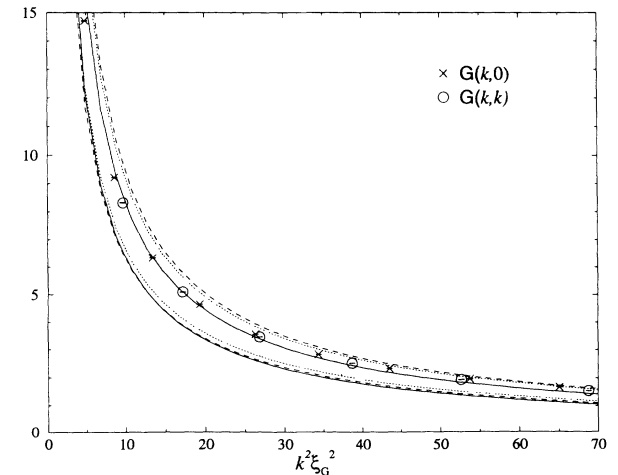


FIG. 16.  $G(k,0)$  and  $G(k,k)$  vs  $k^2 \xi_G^2$  at  $N = 9$  and  $\beta = 0.32$ . The low and high sets of lines (solid, dashed, and dotted) show, respectively, the renormalization group predictions of the standard and the  $\beta_E$  schemes. Solid, dashed, and dotted lines represent, respectively, the lowest, and the one and two next order perturbative solutions.

$$\Lambda_{L,E} = \left( \frac{\Lambda_{L,E}}{M} \right) M = \frac{M}{R_{L,E}} , \quad (170)$$

where  $R$  is the mass- $\Lambda$  parameter ratio in the corresponding scheme, and  $M \equiv 1/\xi_\omega$  is taken from the Monte Carlo simulation.

Again, the best result comes from the  $\beta_E$  scheme, and in particular from its lowest order approximation. The  $\Lambda_E$  parameter shows a similar behavior too, its comparison with the corresponding two-loop formula is already very good, and the  $O(\beta_E^{-1})$  correction does not improve it. This seems to be a general feature of the  $\beta_E$  scheme: Its lowest order renormalization group estimates do not need  $O(\beta_E^{-1})$  corrections, since they are already very good. On the other hand, we should take into account that this scheme comes from a nonperturbative change of variable.

According to the conjectured  $S$  matrix [1-3] and the large  $N$  factorization, two-dimensional (2d)  $SU(N)$  chiral theories should describe free particles in the limit  $N \rightarrow \infty$ . But when considering the two-point Green's function  $G(x)$ , we see that the realization of such physical properties is not trivial at all. Indeed, renormalization group considerations (see Sec. IV) tell us that in the limit  $N \rightarrow \infty$  the asymptotic behavior of  $G(x)$  for  $x \ll 1/M$  is

$$G(x) \sim \ln^2 \left( \frac{1}{xM} \right) , \quad (171)$$

while a free Gaussian Green's function behaves as  $\ln(1/x)$ . Then  $G(x)$ , at small  $x$ , seems to describe the propagation of a composite object formed by two elementary Gaussian excitations, suggesting an interesting hadronization picture:

In the large  $N$  limit, the Lagrangian fields  $U$ , playing the role of noninteracting hadrons, are constituted by two confined particles, which appear free in the large momentum limit, due to asymptotic freedom.

## APPENDIX A

For low-dimensional representations the  $\tilde{z}_{(r)}$  are (known) monomials in  $\beta$ , while their counterparts  $\tilde{z}_{(r+1^N)}$  may be reconstructed starting from the quantities

$$\Gamma_{l_i; m_j} = \left\langle \det U \prod_{i=1}^p \text{Tr} U^{l_i} \prod_{j=1}^q \text{Tr} U^{\dagger m_j} \right\rangle , \quad (A1)$$

which in turn are recursively constructed by applying differential operators and algebraic Schwinger-Dyson equations (Ref. [18], Appendix D) to  $\Gamma_0$ :

$$\Gamma_0 = \tilde{z}_{(1^N)} = J_N(2N\beta) + O(\beta^{3N+2}) . \quad (A2)$$

We have found the general form of a few interesting classes of character coefficients:

$$d_{(l;0)\tilde{z}_{(l;1^N)}} \simeq \sum_{k=0}^l \frac{(N\beta)^{l-k}}{(l-k)!} (-1)^k J_{N+k} , \quad (A3)$$

$$d_{(1^l;0)z_{(1^l;1^N)}} \simeq \frac{(N\beta)^l}{l!} J_N - \frac{(N\beta)^{l-1}}{(l-1)!} J_{N+1} , \quad (A4)$$

$$d_{(0;1^l)z_{(0;1^l+1^N)}} \simeq \sum_{k=0}^l \frac{(N\beta)^{l-k}}{(l-k)!} J_{N-k} , \quad (A5)$$

$$d_{(0;l)z_{(0;l+1^N)}} \simeq \frac{(N\beta)^l}{l!} J_N + \frac{(N\beta)^{l-1}}{(l-1)!} J_{N-1} . \quad (A6)$$

Moreover we have explicitly computed the  $SU(N)$  character coefficients for the first few low-dimensionality representations:

$$d_{(2;0)z_{(2;0)}} \simeq \frac{1}{2}(N\beta)^2 + J_{N+2} + 2N\beta J'_N , \quad (A7)$$

$$d_{(1^2;0)z_{(1^2;0)}} \simeq \frac{1}{2}(N\beta)^2 + J_{N-2} + 2N\beta J'_N , \quad (A8)$$

$$d_{(1;1)z_{(1;1)}} \simeq (N\beta)^2 - 2J_N + 4N\beta J'_N , \quad (A9)$$

$$d_{(3;0)z_{(3;0)}} \simeq \frac{1}{6}(N\beta)^3 + \frac{1}{2}(N\beta)^2 J_{N-1} - \frac{1}{2}(N\beta)^2 J_{N+1} + N\beta J_{N+2} - J_{N+3} , \quad (A10)$$

$$d_{(2,1;0)z_{(2,1;0)}} \simeq \frac{1}{3}(N\beta)^3 + N\beta J_{N-2} + (N\beta)^2 J_{N+1} - (N\beta)^2 J_{N+1} + N\beta J_{N+3} , \quad (A11)$$

$$d_{(1^3;0)z_{(1^3;0)}} \simeq \frac{1}{6}(N\beta)^3 + J_{N-3} + N\beta J_{N-2} + \frac{1}{2}(N\beta)^2 J_{N-1} - \frac{1}{2}(N\beta)^2 J_{N+1} , \quad (A12)$$

$$d_{(2;1)z_{(2;1)}} \simeq \frac{1}{2}(N\beta)^3 + \frac{3}{2}(N\beta)^2 J_{N-1} - 2N\beta J_N + \left[ 1 - \frac{3}{2}(N\beta)^2 \right] J_{N+1} - N\beta J_{N+2} , \quad (A13)$$

$$d_{(1^2;1)z_{(1^2;1)}} \simeq \frac{1}{2}(N\beta)^3 + N\beta J_{N-2} - \left[ 1 - \frac{3}{2}(N\beta)^2 \right] J_{N-1} - 2N\beta J_N - \frac{3}{2}(N\beta)^2 J_{N+1} . \quad (A14)$$

## APPENDIX B

In order to improve our understanding, we briefly considered the Gaussian model, which bears a wide resemblance to the very strong coupling behavior of the chiral models for sufficiently large  $N$ . The Gaussian model is exactly solvable, and one finds that, for arbitrary values of the coupling and arbitrary direction  $\theta$  in the spatial lattice, Eq. (41) becomes [22, 23]

$$\nu(\theta) = m \sqrt{2 + \frac{m^2}{4}} \left[ 1 + \sqrt{1 - m^2(8 + m^2) \left( \frac{\cos 2\theta}{4 + m^2} \right)^2} \right]^{-1/2} \quad (\text{B3})$$

Introducing the auxiliary strong coupling variable

$$\gamma = \frac{1}{4 + m^2} \quad (\text{B4})$$

[related to  $\beta$  by  $\beta = \gamma + O(\gamma^3)$ , odd function of  $\gamma$ ], we obtain

$$\nu(\theta) = \frac{1}{2\gamma} \frac{\sqrt{1 - 16\gamma^2}}{\sqrt{1 + \sqrt{\sin^2(2\theta) + 16\gamma^2 \cos^2(2\theta)}}} ; \quad (\text{B5})$$

that is,  $\nu$  is an odd function of  $\gamma$  for all  $\theta \neq 0$ . The crucial observation however concerns the limit  $\theta \rightarrow 0$ , where

$$\nu(0) = \frac{1}{2\gamma} \sqrt{1 - 4\gamma} , \quad (\text{B6})$$

which is not a function of  $\gamma$  with definite parity. Therefore, while for all  $\theta \neq 0$  the quantity

$$\rho(\theta) = \mu(\theta) + (\cos \theta + \sin \theta) \ln \beta(\gamma) \quad (\text{B7})$$

is an even function of  $\gamma$ , this property does not hold at  $\theta = 0$ . When we consider Green's functions, we recognize that, in strong coupling,

$$G(x_1, x_2) = \beta^{x_1 + x_2} H(x_1, x_2; \beta) , \quad (\text{B8})$$

where  $H$  is always an even function of  $\beta$  (and  $\gamma$ ). As a consequence, the purely kinematical singularity at  $\theta = 0$  in Eq. (B5) prevents the general relationship

$$\rho(\theta) = - \lim_{|x| \rightarrow \infty} \frac{\ln H(x, \beta)}{|x|} \quad (\text{B9})$$

$$C_0(x_1, x_2) = \binom{x_1 + x_2}{x_1} \equiv \binom{x_1 + x_2}{x_2} , \quad (\text{C3})$$

$$\begin{aligned} C_2(x_1, x_2) - C_2(x_1 - 1, x_2) - C_2(x_1, x_2 - 1) \\ = C_0(x_1 - 1, x_2 + 1) + C_0(x_1 + 1, x_2 - 1) - C_0(x_1 - 1, x_2) - C_0(x_1, x_2 - 1) , \end{aligned} \quad (\text{C4})$$

with boundary conditions

$$C_2(x_1, 0) = x_1(x_1 + 1) , \quad C_2(0, x_2) = x_2(x_2 + 1) , \quad (\text{C5})$$

the solution

$$\hat{p}^2 + m^2 = 0 , \quad \hat{p}^2 = 4 \sum_{\mu} \sin^2 \left( \frac{p_{\mu}}{2} \right) , \quad (\text{B1})$$

and is solved by

$$\mu(\theta) = \cos \theta \operatorname{arcsinh}(\nu \cos \theta) + \sin \theta \operatorname{arcsinh}(\nu \sin \theta) , \quad (\text{B2})$$

where

from holding at  $\theta = 0$ . For all other orientations exponentiation can be shown to hold, and in particular the principal diagonal correlation (a quantity of fundamental relevance for tests of rotation invariance) has the proper exponential decay and the corresponding mass gap  $\mu_d$  can be shown to coincide with the value extracted from the diagonal wall-wall correlation:

$$\tilde{G}^{-1} \left( p_1 = \frac{i\mu_d}{\sqrt{2}}, p_2 = \frac{i\mu_d}{\sqrt{2}} \right) = 0 ,$$

$$\mu_d = - \lim_{|x| \rightarrow \infty} \frac{\ln G_{\text{diag}}(x_1 = x_2 = |x|/\sqrt{2})}{|x|} . \quad (\text{B10})$$

Notice that for arbitrary  $\theta$  the two definitions do not strictly coincide.

## APPENDIX C

We could establish the recursive relationships

$$C_0(x_1, x_2) - C_0(x_1 - 1, x_2) - C_0(x_1, x_2 - 1) = 0 , \quad (\text{C1})$$

with boundary conditions

$$C_0(x_1, 0) = C_0(0, x_2) = 1 \quad (\text{C2})$$

the (well-known) solution

$$C_2(x_1, x_2) = \binom{x_1 + x_2}{x_1} \left[ \frac{x_1(x_1 + 1)}{x_2 + 1} + \frac{x_2(x_2 + 1)}{x_1 + 1} \right], \quad (C6)$$

$$\begin{aligned} C_4(x_1, x_2) - C_4(x_1 - 1, x_2) - C_4(x_1, x_2 - 1) \\ = C_2(x_1 + 1, x_2 - 1) + C_2(x_1 - 1, x_2 + 1) - C_2(x_1, x_2) + C_0(x_1 + 2, x_2 - 1) \\ + C_0(x_1 - 1, x_2 + 2) + C_0(x_1, x_2 - 2) + C_0(x_1 - 2, x_2) - 3C_0(x_1, x_2), \end{aligned} \quad (C7)$$

with boundary conditions

$$C_4(x_1, 0) = \frac{x_1^2(x_1 + 1)^2}{4} + \frac{x_1(x_1 + 1)}{2} + 4x_1, \quad C_4(0, x_2) = \frac{x_2^2(x_2 + 1)^2}{4} + \frac{x_2(x_2 + 1)}{2} + 4x_2, \quad (C8)$$

and the solution

$$\begin{aligned} C_4(x_1, x_2) = \binom{x_1 + x_2}{x_1} \left[ x_1 x_2 + 2x_1 + 2x_2 + \frac{x_2(x_2 + 3)}{x_1 + 1} + \frac{x_1(x_1 + 3)}{x_2 + 1} \right. \\ \left. + \frac{(x_2 - 1)x_2(x_2 + 1)(x_2 + 2)}{2(x_1 + 1)(x_1 + 2)} + \frac{(x_1 - 1)x_1(x_1 + 1)(x_1 + 2)}{2(x_2 + 1)(x_2 + 2)} - \frac{2x_1 x_2}{x_1 + x_2} \right]. \end{aligned} \quad (C9)$$

The function  $B$  can be computed by the relationship

$$B(x_1, x_2) = \sum_a a C_0^{(a)}(x_1, x_2), \quad (C10)$$

where  $C_0^{(a)}(x_1, x_2)$  is the number of minimal self-avoiding paths connecting the origin with  $x$  and forming  $a$  right angles.  $C_0^{(a)}$  satisfies the normalization condition

$$\sum_a C_0^{(a)}(x_1, x_2) = C_0(x_1, x_2). \quad (C11)$$

Solving appropriate recursive equations it is possible to prove that

$$\begin{aligned} \sum_{x_1, x_2} C_0^{(a)}(x_1, x_2) t_1^{x_1} t_2^{x_2} &= \left( \frac{t_1}{1 - t_1} + \frac{t_2}{1 - t_2} \right) \left( \frac{t_1 t_2}{(1 - t_1)(1 - t_2)} \right)^{\frac{a}{2}} \quad \text{for even } a, \\ \sum_{x_1, x_2} C_0^{(a)}(x_1, x_2) t_1^{x_1} t_2^{x_2} &= 2 \left( \frac{t_1 t_2}{(1 - t_1)(1 - t_2)} \right)^{\frac{a+1}{2}} \quad \text{for odd } a, \end{aligned} \quad (C12)$$

and, as a consequence,

$$\sum_{x_1, x_2} B(x_1, x_2) t_1^{x_1} t_2^{x_2} = \frac{2t_1 t_2}{(1 - t_1 - t_2)^2}. \quad (C13)$$

We then trivially obtain

$$B(x_1, x_2) = \frac{2x_1 x_2}{x_1 + x_2} C_0(x_1, x_2). \quad (C14)$$

#### APPENDIX D

We report here the  $N = \infty$  strong coupling series of some relevant quantities:

$$E = 1 - \beta - 2\beta^3 - 6\beta^5 - 38\beta^7 - 240\beta^9 - 1812\beta^{11} - 14126\beta^{13} + O(\beta^{15}), \quad (D1)$$

$$\chi = 1 + 4\beta + 12\beta^2 + 36\beta^3 + 100\beta^4 + 284\beta^5 + 796\beta^6 + 2276\beta^7 + 6444\beta^8 + 18572\beta^9 + 53292\beta^{10} + O(\beta^{11}), \quad (D2)$$

$$Z_G = \beta^{-1} [1 - \beta^2 - 6\beta^4 - 4\beta^5 - 20\beta^6 - 24\beta^7 - 148\beta^8 - 216\beta^9 + O(\beta^{10})], \quad (D3)$$

$$M_G^2 = \beta^{-1} [1 - 4\beta + 3\beta^2 + 2\beta^4 - 4\beta^5 + 12\beta^6 - 40\beta^7 + 84\beta^8 - 296\beta^9 + O(\beta^{10})] , \quad (\text{D4})$$

$$\mu_{\text{side}} = -\ln \beta - 2\beta - \frac{2}{3}\beta^3 - 2\beta^4 - \frac{42}{5}\beta^5 - 8\beta^6 - \frac{310}{7}\beta^7 - 70\beta^8 + O(\beta^9) , \quad (\text{D5})$$

$$\mu_{\text{diag}} = \sqrt{2} [-\ln 2\beta - \beta^2 - 3\beta^4 - \frac{119}{6}\beta^6 + O(\beta^8)] . \quad (\text{D6})$$

- 
- [1] E. Abdalla, M. C. B. Abdalla, and A. Lima-Santos, Phys. Lett. **140B**, 71 (1984).
- [2] P. Wiegmann, Phys. Lett. **141B**, 217 (1984).
- [3] P. Wiegmann, Phys. Lett. **142B**, 173 (1984).
- [4] P. Rossi and E. Vicari, Phys. Rev. D **49**, 1621 (1994).
- [5] J. Balog, S. Naik, F. Niedermayer, and P. Weisz, Phys. Rev. Lett. **69**, 873 (1992).
- [6] A. M. Polyakov, *Gauge Fields and Strings* (Harwood Academic, New York, 1988).
- [7] G. Parisi, in *High Energy Physics—1980*, Proceedings of the XXth International Conference on High Energy Physics, Madison, Wisconsin, 1980, edited by L. Durand and L. Pondrom, AIP Conf. Proc. No. 68 (AIP, New York, 1981).
- [8] P. Rossi and E. Vicari, in *Lattice '93*, Proceedings of the International Symposium, Dallas, Texas, 1993 [Nucl. Phys. B (Proc. Suppl.) (in press)].
- [9] M. Falcioni, E. Marinari, M. L. Paciello, G. Parisi, and B. Taglienti, Phys. Lett. **102B**, 270 (1981); **108B**, 331 (1982).
- [10] I. Bars and F. Green, Phys. Rev. D **20**, 3311 (1979).
- [11] S. Samuel, J. Math. Phys. **21**, 2695 (1980).
- [12] I. Bars, J. Math. Phys. **21**, 2678 (1980).
- [13] R. C. Brower, P. Rossi, and C. I. Tan, Phys. Rev. D **23**, 942 (1981).
- [14] M. Creutz, J. Math. Phys. **19**, 2043 (1978).
- [15] J. Shigemitsu and J. B. Kogut, Nucl. Phys. **B190**, 365 (1981).
- [16] R. C. Brower, P. Rossi, and C. I. Tan, Nucl. Phys. **B190**, 699 (1981).
- [17] F. C. Hansen, "SU(N) Haar Measure Integrals in the Nonlinear  $\sigma$  Model", Report No. BUTP-90/42 (unpublished).
- [18] F. Green and S. Samuel, Nucl. Phys. **B190**, 113 (1981).
- [19] P. Rossi, Phys. Lett. **117B**, 72 (1982).
- [20] A. Guha and S. C. Lee, Nucl. Phys. **B240**, 141 (1984).
- [21] E. Barsanti and P. Rossi, Z. Phys. C **36**, 143 (1987).
- [22] V. F. Muller, T. Raddatz, and W. Ruhl, Nucl. Phys. **B251**, 212 (1985); **B259**, 745(E) (1985).
- [23] M. Campostrini and P. Rossi, Riv. Nuovo Cimento **16**, 1 (1993).
- [24] H. Kawai, R. Nakayama, and K. Seo, Nucl. Phys. **B189**, 40 (1981).
- [25] Y. Brihaye and P. Rossi, Nucl. Phys. **B235**, 226 (1984).
- [26] M. Falcioni and A. Treves, Nucl. Phys. **B265**, 671 (1986).
- [27] M. Campostrini and P. Rossi, Phys. Lett. B **242**, 225 (1990).
- [28] S. Hikami, Phys. Lett. **98B**, 208 (1980).
- [29] A. McKane and M. Stone, Nucl. Phys. **B163**, 169 (1980).
- [30] N. Cabibbo and E. Marinari, Phys. Lett. **119B**, 387 (1982).
- [31] R. Petronzio and E. Vicari, Phys. Lett. B **254**, 444 (1991).
- [32] A. D. Kennedy and B. J. Pendleton, Phys. Lett. **156B**, 393 (1985).
- [33] F. Karsch and R. Petronzio, Phys. Lett. B **139**, 403 (1984).
- [34] U. Wolff, Phys. Lett. B **248**, 335 (1990).
- [35] M. Campostrini, P. Rossi, and E. Vicari, Phys. Rev. D **43**, 4643 (1992).